Optimal preparation of low-cost and high-permeation NaA zeolite membrane for effective ethanol dehydration

F.Z. Charik, B. Achiou, A. Belgada, Z.C. Elidrissi, M. Ouammou, M Rabiller-Baudry, S.A. Younssi

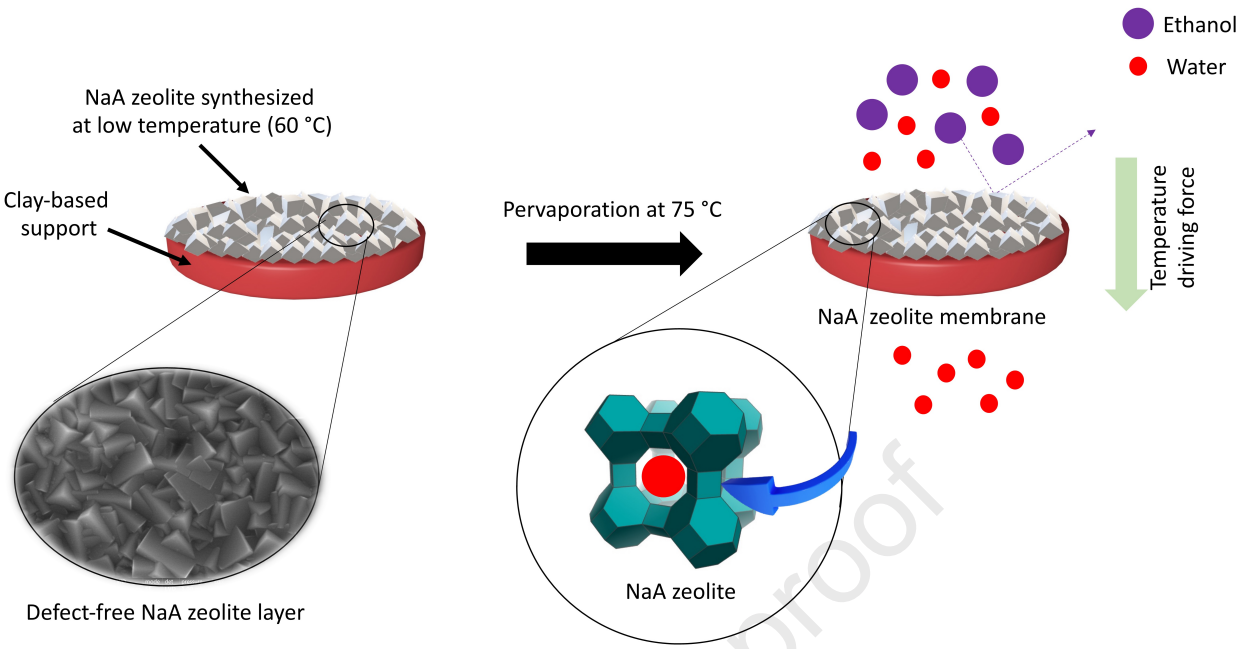

Optimal preparation of low-cost and high-permeation NaA zeolite membrane for effective ethanol dehydration

Fatima Zohra Charik [*1,2], Brahim Achiou [1], Abdessamad Belgada [1], Zakarya Chafiq Elidrissi[1], Mohamed Ouammou [1], Murielle Rabiller-Baudry [2], Saad Alami Younssi [1],

[1] Laboratory of Materials, Membranes and Environment, Faculty of Sciences and Technologies of Mohammedia, Hassan II University of Casablanca, Morocco

[2] Univ Rennes, CNRS, ISCR (Institut des Sciences Chimiques de Rennes) - UMR 6226, F-35000, Rennes, France

Corresponding author *: fatimazohra.charik-etu@etu.univh2c.ma

Abstract

In this work, low-cost and high permeation NaA zeolite membrane was successfully prepared on kaolinite support by in-situ crystallization using secondary growth method. The effect of synthesis conditions including temperature and time of crystallization, and water ratio was studied aiming to improve the quality and the performance of the membrane. The prepared membrane was thoroughly characterized using many techniques such as X-ray diffraction, scanning electron microscopy infrared spectroscopy, Brunauer-Emmett-Teller specific surface area and zeta potential to investigate the layer deposition. The prepared membrane exhibits high permeation flux of 8.49 kg m $^{-2}$ h^{-1} and separation factor of 10900 for the dehydration of 90 wt.% ethanol by pervaporation at 75 °C.

Keywords: low-cost membrane; zeolite material; clay; hydrothermal synthesis; pervaporation.

1. Introduction

For decades, membrane-based processes have gained a great success in the separation of compounds at molecular scale. Membrane processes present several advantages like high energy efficiency and low maintenance process **[1,2]**. Two main classes of materials are used in the manufacture of membranes including organic and inorganic materials. Particularly, ceramic materials display more features than polymeric materials in terms of chemical, thermal and mechanical stability **[3]**. Furthermore, ceramic membranes are more resistant to the fouling compared to polymer-based membranes. However, the high cost of commercial ceramic materials limits their use in membrane technology.

In recent years, geomaterials have been introduced in the preparation of inorganic membranes and showed promising results especially in microfiltration (MF) **[4–7]** ultrafiltration (UF) **[8,9]**. Moreover, geomaterials offer several advantages like cost reduction and energy saving. For instance, the cost of commercial ceramic materials can be reduced from 500-1000 \$ m^{-2} for alumina tubular membrane to 25.5 \$ m^{-2} for clay-based membrane **[10]**.

Among inorganic materials, zeolites are considered as promising materials that are used in the preparation of membranes and own unique properties counting uniform micropores, molecular sieving effect, thermal stability, mechanical resistance, adsorption and ion exchange properties **[1,11]**. Due to these specific characteristics, zeolites can be used in a wide range of applications in liquid and gas separation.

Several types of zeolites have been discovered up to now possessing different framework structures. Zeolites with small pore sizes like linda type A (LTA) and chabazite (CHA) are the most suitable for many separation processes such as gas separation and solvent dehydration. LTA zeolite is distinguished by a pore size of 0.4 nm, Si/Al ratio of 1 and hydrophilic character which allows a strong interaction with polar molecules like water **[12]**. This zeolite is the most appropriate for the dehydration of solvents like ethanol and methanol, because the pore size of

the zeolite is larger than that of water molecule estimated to be 0.28 nm and smaller than the majority of organic compounds **[13]**.

Pervaporation (PV) has been recognized as an energy-saving process for the separation of azeotropic mixtures compared to other technologies notably distillation and evaporation **[9,11]**. Typically, PV process takes place in three successive steps: (i) adsorption of species onto the membrane (liquid phase), (ii) diffusion through the membrane (iii) desorption of species (vapor phase). The dehydration of organics especially alcohols is considered as the potential application of PV.

Several factors are responsible for the preparation of high-quality zeolite membranes including time and temperature of crystallization, composition of synthesis batch, seeding method, etc. **[13]**. It is well-known that the time of crystallization controls the thickness of the membrane, while the temperature of crystallization can induce a phase transformation of the zeolite structure. Thus, it is important to consider the effect of each parameter during the preparation of zeolite membrane.

Lee et al. reported that the increase in synthesis time promotes the crystallinity of obtained zeolite **[17]**. It was found that the optimal synthesis time of crystallization of NaA zeolite membrane was 24 h. This is in good agreement with the results reported by *Achiou et al.* that also prepared a defect-free NaA zeolite membrane during 24 h of crystallization time **[15]**. Furthermore, it was shown that increasing time from 24 to 48 h leads to aging of zeolite crystals. On the other hand, varying the crystallization temperature from 60 to 80 °C involves the formation of zeolite type P phase **[15]**. *Liu et al*. studied also the variation of synthesis temperature from 100 to 130 °C for a Si-rich LTA membrane. It was reported that the increase in temperature of over 120 °C favors the crystallization of CHA zeolite **[16]**.

In this study, a cost-effective zeolite membrane was prepared using clay-based support. The deposition of NaA zeolite layer was achieved by secondary growth method. Firstly, the

influence of synthesis parameters including temperature and time of crystallization and water ratio in the gel composition on the morphology, crystallinity, permeation flux and selectivity of the membrane was investigated. Secondly, the optimal prepared membrane was tested for the dehydration of 90 wt.% ethanol, varying the water content in the feed and the operating temperature during dehydration experiments.

2. Experimental

2.1. Chemicals and materials

Chemicals used in this study include sodium hydroxide (NaOH, 98 wt.%), sodium aluminate ($NaAlO_2$, 50-56 wt.% of Al_2O_3) as Al source, sodium silicate (Na_2O_3Si. $9H_2O$ powder (Meta), extra pure) as Si source, were purchased from Sigma Aldrich. Absolute ethanol (CH_3CH_2OH, 99.9 wt.%) used in pervaporation experiments was provided by Biosmart. Water used for the membrane preparation and in the PV experiment is double distilled water.

Ceramic substrate with diameter of 37.8 mm and thickness of 2.0 mm was made from kaolinite. Furthermore, it has a porosity of 12.3%, pore size of 2.0 μm and mechanical strength of 23.3 MPa. Further details of kaolinite substrate are reported elsewhere **[5]**.

2.2. Synthesis of NaA zeolite powder

Synthesis batch of NaA zeolite powder was obtained by mixing sodium aluminate, sodium silicate, sodium hydroxide and water according to the molar composition of Al_2O_3: 2 SiO_2: 15 Na_2O: 400 H_2O. Firstly, sodium hydroxide was dissolved in water, then sodium silicate was added and stirred under 200 rpm until entire solubilization to obtain solution S1. Similarly, sodium aluminate was added to sodium hydroxide dissolved in water to obtain solution S2. Secondly, S1 was poured into S2 under strong stirring. The mixture was aged at room temperature for 1 h. The prepared hydrogel was hydrothermally treated in Teflon autoclave at 60 °C for 24 h. After hydrothermal process, the obtained powder was centrifuged at 5000 rpm

and washed with water several times until pH is less than 8. The final product was dried in oven at 60 °C for 24 h.

2.3. Preparation of NaA zeolite membrane

Prior to hydrothermal synthesis, the kaolinite substrate was handily polished using abrasive paper P600 to reduce the roughness of the surface. Later, the support was washed with water at room temperature and dried overnight in oven at 60 °C. Thereafter, one face of the support was masked to prevent the crystallization on the two faces of the support during hydrothermal synthesis. The other face of kaolinite substrate was seeded with NaA zeolite powder previously synthesized in **Section 2.2**.

NaA zeolite membrane was hydrothermally synthesized using secondary growth method. The synthesis solution was prepared similarly to that of NaA zeolite powder. The seeded kaolinite support was immersed in the batch solution and placed in a vertical way in the autoclave. This latter was placed in oven to be treated under hydrothermal conditions. The effect of hydrothermal parameters on the preparation of NaA zeolite membrane was investigated. The crystallization temperature was varied from 60 to 90 °C, while the crystallization time was increased from 6 to 24 h, and the water content was varied in the batch composition Al_2O_3: 2 SiO_2: 15 Na_2O: x H_2O, where *x* is equal to 200, 400 or 600. After hydrothermal treatment, the membrane was removed from the autoclave and then washed with water repeatedly to remove hydroxide sodium traces. Finally, the obtained membrane was dried in oven at 60 °C. **Fig. 1** presents the preparation process of the zeolite membrane.

Fig. 1. Preparation process of the NaA zeolite membrane.

2.4. Pervaporation

The prepared membrane was applied for the separation of 90 wt.% ethanol/water mixture via PV process. Briefly, the prepared membrane was placed in a stainless-steel module. The feed solution with desired concentration of ethanol and water was poured into the vessel. A

circulating pump helps the solution to circulate in the close system. The feed solution was heated using a Marie bath in order to attend the desired PV temperature. Due to N_2 cold trap, the vapor permeate was collected under a pressure of 0.5 mbar using vacuum pump **[19].** During each experiment, the permeate was weighted and analyzed to determine the flux (Kg m^{-2} h^{-1}) and separation factor according to **Eq. (1)** and **Eq. (2)** respectively.

$$J = \frac{m}{A \times t} \qquad (1)$$

$$\alpha = \frac{\frac{Yw}{Yeth}}{\frac{Xw}{Xeth}} \qquad (2)$$

Where m is the weight of the collected permeate given in Kg, A is the surface area of the membrane given in m^2, and t is the time of experiment given in h. While, X_w and Y_w are respectively the weight fractions of water in the feed and permeate, and X_{eth} and Y_{eth} are the weight fractions of ethanol in the permeate and feed respectively.

2.5. Characterizations of synthesized zeolite and prepared membrane

X-ray diffraction (XRD) was used to determine the crystallinity and purity of the synthesized NaA zeolite powder using the diffractometer Philips X'PERT PRO anticathode with Cu-Kα radiation source (λ= 1.5406 Å) in the 2θ range from 5 to 90 °C. The specific surface area of NaA zeolite powder was measured by Brunauer-Emmett-Teller (BET) nitrogen adsorption using Quantachrome TouchWin 1.2x,NOVAtouch. Infrared spectroscopy (FTIR) analysis was carried out to confirm the chemical structure and groups present in zeolite powder. The analysis was performed with the spectrometer Affinity-1S SHIMADZU equipped with a golden gate single reflection ATR accessory. The spectrum was recorded in the interval of 4000-500 cm^{-1}. Zeta potential measurements were carried out to determine the surface charge of the NaA zeolite powder. The analysis was performed with the instrument Anton Paar GmbH,Graz owning an Ag/AgCl electrode in the pH range 4-10. The pH was adjusted by using NaOH and HCL solutions. The given value of zeta potential is the average of 20 measurements.

Scanning Electron Microscopy (SEM) was utilized to examine the morphology of prepared membranes with a Quattro S, FEG FEI scanning electron microscope. Membrane hydrophobicity was determined by the measurements of water and ethanol contact angle via TRACKER contact angle instrument using the sessile drop method.10 measurements were carried out in various points at the surface of the sample. The resulting value is the average of the 10 measurements. Gas chromatography was used to determine the concentration of ethanol and water in feed and permeate using the instrument Agilent 7890 A GC.

3. Results and discussion

3.1. Characterization of NaA zeolite powder

Fig. 2 displays XRD patterns of the synthesized NaA zeolite powder. It should be noted that the pattern belongs to the synthesized NaA zeolite powder with water ratio of 400 at 60 °C, 24h. As it can be seen from the figure, all peaks are matched with that of NaA zeolite. This means that high-quality NaA zeolite was synthesized at lower temperature. **Fig. 3** shows the FTIR spectrum of synthesized zeolite powder. The characteristic bands of NaA zeolite are expected to be detected in the range 1200-400 cm^{-1} **[20].** The band at 630 cm^{-1} refers to symmetric stretching assigned to the internal T-O-T bond (T=Si, Al) while the band at 1000 cm^{-1} is attributed to the asymmetric stretching of T-O-T bond. The band at 570 cm^{-1} corresponds to the internal vibration of the bending (Si, Al)-O **[21]**. The band appearing at 1625 cm^{-1} belongs to the bending mode of OH groups including undissociated molecular water. The bands at 3475 and 3700 cm^{-1} correspond to the stretching vibration of OH groups **[22]**. N_2 adsorption-desorption was performed at 77 K. **Fig. 4** shows the adsorption and desorption isotherms of the synthesized NaA zeolite powder. According to the classification of The International Union of Pure and Applied Chemistry (UIPAC), the isotherms correspond to type V adsorption. The specific surface area of NaA zeolite powder was found to be 6.77 $m^2\ g^{-1}$.

The surface charge of NaA zeolite powder depends on the number of hydroxyl groups on the surface **[23].** When pH increases, the zeta potential value becomes more negative due to the increase of deprotonation of hydroxyl groups. Zeta potential of NaA zeolite powder was found to be positive with a value of 28 mV when the pH equals to 4. The surface charge remains positive up to a pH of 8, and then turns into a negative value of -48 when the pH equals to 10 as shown in **Fig. 5.** The isoelectric point was found to be 8.58, and at this pH the potential zeta is null due to neutralization of all acidic sites of NaA zeolite **[23]**.

Fig. 2. XRD pattern of synthesized zeolite powder.

Fig. 3. ATR-FTIR of synthesized zeolite powder.

Fig. 4. N_2 adsorption and desorption of zeolite powder at 77 K.

Fig. 5. Zeta potential of zeolite powder.

3.2. Characterization of NaA zeolite membrane

In this section, the effect of the main synthesis parameters was studied including the temperature and time of crystallization, and water ratio in the batch synthesis. Furthermore, the water and ethanol contact angle were measured for the optimal membrane.

3.2.1. Role of crystallization temperature

SEM images of NaA membrane prepared at different crystallization temperatures are shown in **Fig. 6**. At 60 °C, only cubic crystals of NaA zeolite are clearly observed on the membrane surface with absence of surface defects like cracks and pinholes. At 80 °C, it can be seen that there is another zeolite phase coexisting with NaA zeolite crystals that is zeolite type P phase with walnut-like structure. This results from the high applied temperature that favors the crystallization of zeolite type P. Similarly, *Achiou et al.* described the coexistence of zeolite P with NaA zeolite when the crystallization occurs at temperature of 80 °C **[15]**. When the temperature was increased to 90 °C, zeolite type P crystals could not be obtained and NaA zeolite crystals were hardly observed on the surface of the membrane. Therefore, the optimal

temperature of crystallization of NaA zeolite was fixed at 60 °C. This temperature is the most likely to form well-shaped zeolite crystals, and hence a good quality zeolite layer.

Fig. 6. Top-view SEM images of the prepared NaA zeolite membranes at different crystallization temperatures (a) 60 °C (b) 80 °C and (c) 90 °C, at crystallization time of 24 h and a composition of 1 Al_2O_3: 2 SiO_2: 15 Na_2O: 400 H_2O.

3.2.1.2. Role of crystallization time

Fig. 7 shows SEM images of prepared membranes at different crystallization times. At a synthesis time of 6 h, the cubic shape of NaA crystals could not be obtained. The crystals started to grow. Besides, the surface of the membrane presents some pinholes. When crystallization time was increased to 12 h, NaA crystals completely cover the surface of the substrate and have a well-defined cubic shape with sizes ranging from 0.5 to 2.9 μm. Similarly, after 24 h of crystallization, the zeolite layer is completely and homogeneously grown on kaolinite support. The size of crystals is relatively uniform all along the zeolite layer. The more the synthesis time increases the more the zeolite layer becomes thicker. The thickness of the prepared membrane varies from 2.99 to 7.47 μm when crystallization time increases from 6 to 24 h respectively. This result confirms that the synthesis time controls the thickness of the zeolite layer. These results suggest that 6 h is not sufficient for the formation of NaA zeolite layer. 12 h of crystallization is enough for obtaining a well-grown zeolite layer. However, the zeolite crystals obtained at 24 h have more uniform aspect than those obtained at 12 h.

Fig. 7. Top and cross-view SEM images of prepared NaA zeolite membrane at different crystallization times (a,b) 6 h (c,d) 12 h (e,f) 24 h at 60 °C and a composition of 1 Al_2O_3: 2 SiO_2: 15 Na_2O: 400 H_2O.

3.2.1.3. Role of water ratio

Water ratio was investigated from 200 to 600, at a crystallization temperature of 60 °C and a crystallization time of 24 h. Typically, the concentration of the gel has an impact on the

continuity and homogeneity of the formed zeolite layer. With a ratio of 200, the higher concentration of the gel leads to the formation of a dense layer, as it can be seen in **Fig. 8**. By increasing the ratio to 600, the formed zeolite layer is not dense and non-continuous because of the weak concentration of the gel. Thus, the nucleation and growth of zeolite crystals are not promoted on the membrane surface. On the other hand, the thickness of zeolite layer decreases with the increase of the water content in the synthesis batch. Therefore, water content could affect the permeation flux. Same observations were reported by *Shirazien et al.* **[24]** stating that a concentrated gel leads to the formation of a thicker zeolite layer. Moreover, defects like pinholes are likely to form on the membrane when the gel is more concentrated. In previous work, it was reported that increasing the water ratio to over 1000 allows to obtain an amorphous phase with the absence of zeolite crystals **[17]**. On the other hand, decreasing water ratio to less than 200 favors the formation of the sodalite (SOD) phase because the low content of water induces a high concentration of sodium ions **[17]**.

To sum up, the optimal conditions to prepare NaA zeolite membrane free from defects are 60 °C of crystallization temperature, 24 h of crystallization time and 400 of water ratio. This membrane was subjected to further characterization and PV experiments.

Fig. 8. Top and cross-view SEM images of prepared NaA zeolite membrane at different water ratios of (a,b) 200 (c,d) 400 (e,f) 600 at 60 °C and 24 h of crystallization.

3.2. 2. Contact angle measurements of optimized membrane

Contact angle is considered the main factor to take into account to investigate membrane wettability. A contact angle superior to 90° describes a hydrophobic character of the membrane surface. Whereas, a contact angle less than 90° is related to a hydrophilic surface. Contact angle measurements of water and ethanol for kaolinite support and NaA zeolite membrane are given in **Fig. 9**. Kaolinite support has a water contact angle of 29.13° which means that it has a hydrophilic character. Contact angle of ethanol at the support surface is about 0° which means

that the ethanol droplet spreads very fast when in contact with the support. For NaA zeolite membrane, water contact angle was found to be 72.20°, indicating that the NaA zeolite membrane has a low hydrophilicity. Whereas, for ethanol the membrane displays a contact angle of 12.83°.

Fig. 9. Contact angle measurements of water and ethanol for kaolinite support and NaA zeolite membrane prepared at 60 °C, 24 h and a composition of 1 Al_2O_3: 2 SiO_2: 15 Na_2O: 400 H_2O.

3.3. Separation performance of NaA zeolite membrane

The optimized membrane was applied for ethanol dehydration via PV process. In this study, the effect of water content in the feed solution on membrane selectivity and flux was studied varying the percentage of water from 10 to 40 wt.%. The operating temperature was also investigated from 60 to 80 °C.

3.3.1. Effect of PV temperature

The temperature of PV has a great contribution to the membrane flux. The temperature controls the diffusivity and adsorption of species during PV **[25]**. PV temperature was varied from 60 to 80 °C to evidence the impact on transfer of species. **Fig. 10** depicts the evolution of permeation flux and separation factor as a function of the operating temperature. The permeate flux seems to increase with the increase of PV temperature from 60 to 80 °C. This could be explained by the solution-diffusion mechanism that governs the transport of water through NaA zeolite membrane **[26]**. The diffusivity of water increases when the temperature of PV was fixed at 80 °C leading to the highest permeate flux. Moreover, it is reported elsewhere **[25]** that the partial pressure of compounds increases when the PV temperature exceeds the boiling point of compounds resulting in the improvement of the driving force. Thus, the transport of species is enhanced which means that the permeate flux could increase. From the other side, the separation factor keeps its high value of over 10000 when the feed temperature increases due to the water

permeation that is also boosted at elevated temperatures **[27]**. In other words, water molecules are more easily diffusing in zeolite pores than ethanol molecules **[28]**. The relationship between temperature and flux can be expressed by Arrhenius equation **(Eq. (3)) [29]**.

$$\ln(\frac{J}{\Delta Pi}) = \frac{-Ea}{\mathrm{R}}\ \frac{1}{T} \qquad (3)$$

Where J is the permeation flux, ΔPi (mbar) is the pressure difference between the feed and the permeate, T is the operating temperature (K) and R is the gas constant (J mol^{-1} K^{-1}). The activation energy can be deduced from the plot of ln (J/ΔPi) vs. 1/T. From **Fig. 11,** it can be seen that the water and ethanol have an activation energy of -68.40 $kJ.mol^{-1}$ and -57.88 $kJ.mol^{-1}$ respectively, which means that ethanol requires more energy to diffuse than water **[30]**.

Fig. 10. Effect of operating temperature on membrane flux and separation factor for the dehydration of 90 wt.% ethanol.

Fig. 11. Arrhenius plot of water and ethanol permeances.

3.3.2. Effect of water content in the feed

The effect of water content on the separation performance of the prepared membrane was also studied. Water content was varied from 10 to 40 wt.%. The PV temperature was maintained constant at 75 °C. **Fig. 12** shows the variation of the permeate flux versus the water content. As it can be seen, permeate flux is enhanced with increasing water content from 10 to 40 wt.%. This could be explained by the increase of the water flux when the concentration of ethanol decreases due to the increase of adsorption capacity of water **[31]**. At high water content, water molecules prevent other permeate species to pass through the membrane. Water molecules have the ability to adsorb into zeolites pores as their size is smaller than NaA zeolite pore. The transport of water consists in the accumulation of water molecules on the interface of the membrane, then the diffusion of the species through the membrane takes place due to concentration-dependent diffusivities. Finally, the molecules are desorbed from the permeate side. The separation factor of the prepared membrane slightly drops when the water content

increases. The separation factor for 10 and 30 wt.% of water is still over 10000, which approves the high separation ability of the prepared membrane.

Fig. 12. Variation of permeation flux as a function of water content in water/ethanol mixture at 75 °C.

3.4. Cost estimation of NaA zeolite membrane

To give an estimation of the membrane cost, it is necessary to take into consideration raw materials price and energy consumption. The cost estimation of the prepared NaA membrane is divided into two parts: the cost estimation of kaolinite support and zeolite layer, separately. The given estimations in **Table 1** concern the manufacture of kaolinite support and NaA zeolite layer. **Table 1** gives the contribution cost of raw materials and energy consumption of both support and membrane layer. The electricity cost was calculated using **Eq. (4) [32]**.

$$Electricity\ cost = \frac{operating\ time\ (h) * load\ (Kwh) * unit\ charge\ (\$/Kwh)}{\text{unit area (}\ m^2)} \qquad \textbf{(4)}$$

The estimated cost for the preparation of kaolinite support was found to be 18.63 \$ m^{-2} including the price of raw materials, crushing, sieving and sintering. This demonstrates that kaolinite support satisfies the property of low-cost support because it is less than some other clay-based membranes reported in the literature as shown in **Table 2.**

The cost of deposited NaA zeolite layer was estimated to be 90.91 \$ m^{-2} including price of raw materials and energy consumption. Hence, the total cost of the prepared membrane is equal to 110 \$ m^{-2}. In general, the average cost of zeolite membrane was reported to be 2300 € m^{-2} (≈2345 \$ m^{-2}) including a full-module design **[33]**. 80-90% of the cost is reserved to the module and the support, while the zeolite layer only constitutes the smallest part. Which indicates that the cost of the zeolite membrane is reduced by the use of low-cost support. The cost of the prepared NaA zeolite membrane is reduced by the use of inexpensive kaolinite support compared to commercial inorganic membranes (500 \$ m^{-2}). Therefore, the cost of the prepared zeolite membrane could be comparable to the cost of polymeric membranes (200 \$ m^{-2}) **[33].**

Table 1

Estimation cost of kaolinite support and NaA zeolite layer.

Table 2

Comparison of preparation cost of clay-based membranes.

4. Conclusion

In this work, NaA zeolite membrane was successfully prepared on ceramic kaolinite support via hydrothermal method using secondary growth process. The crystallization time controls the thickness and the growth of NaA zeolite layer, while the crystallization temperature impacts the formation of the NaA zeolite phase. Water ratio in the batch synthesis influences the continuity and homogeneity of the formed zeolite layer. The optimal membrane was prepared at 60 °C, 24 h and a water ratio of 400. These conditions lead to the preparation of defect-free NaA membrane. The optimized membrane shows excellent results for the separation of ethanol/water mixture. The flux was found to be 8.49 kg m^{-2} h^{-1} and the separation factor is over 10000. The membrane cost was estimated to be 110 \$ m^{-2} which makes this membrane cheaper than available commercial membranes. This is could be promising for industrial application.

Declaration of competing interest

The authors declare that they do not have any personal relationships or financial problems that could influence the work.

CRediT Authors contribution

F.Z. Charik: Writing-original draft, **B. Achoiu:** Review and Editing, **A. Belgada:** Writing-original draft, **Z. Chafiq El Idrissi:** Writing- original draft, **M. Ouammou:** Validation, **M. Rabiller-Baudry:** Supervision, **S. Alami Younssi:** Supervision

Acknowledgments

This work was supported by MESRSI (Ministère de l'Enseignement Supérieur et de la Recherche Scientifique et de l'Innovation) and CNRST (Centre National pour la Recherche

Scientifique et Technique-Morocco) (Project : PPR/2015/72). Fatima Zohra Charik acknowledges Eiffel & Campus France for the PhD grant n°EIFFEL-DOCTORAT 2020/n°P757215H.

References

[1] D. Meng, X. Kong, X. Tang, W. Guo, S. Yang, Y. Zhang, H. Qiu, Y. Zhang, Z. Zhang, Thin SAPO-34 zeolite membranes prepared by ball-milled seeds, Sep. Purif. Technol. 274 (2021) 118975. https://doi.org/10.1016/j.seppur.2021.118975.
[2] M. Breida, S. Alami Younssi, M. Ouammou, M. Bouhria, M. Hafsi, Pollution of Water Sources from Agricultural and Industrial Effluents: Special Attention to NO_3^-, Cr(VI), and Cu(II), in: M. Eyvaz, E. Yüksel (Eds.), Water Chem., IntechOpen, 2020. https://doi.org/10.5772/intechopen.86921.
[3] H. Elomari, B. Achiou, D. Beqqour, K. Khaless, R. Beniazza, M. Ouammou, A. Aaddane, S. Alami Younssi, R. Benhida, Preparation and characterization of low-cost zirconia/clay membrane for removal of acid orange 74 dye, Mater. Today Proc. (2021) S2214785321027760. https://doi.org/10.1016/j.matpr.2021.03.674.
[4] A. Belgada, F.Z. Charik, B. Achiou, T. Ntambwe Kambuyi, S. Alami Younssi, R. Beniazza, A. Dani, R. Benhida, M. Ouammou, Optimization of phosphate/kaolinite microfiltration membrane using Box–Behnken design for treatment of industrial wastewater, J. Environ. Chem. Eng. 9 (2021) 104972. https://doi.org/10.1016/j.jece.2020.104972.
[5] O. Samhari, S. Alami Younssi, M. Rabiller-Baudry, P. Loulergue, M. Bouhria, B. Achiou, M. Ouammou, Fabrication of flat ceramic microfiltration membrane from natural kaolinite for seawater pretreatment for desalination and wastewater clarification, Desalination Water Treat. 194 (2020) 59–68. https://doi.org/10.5004/dwt.2020.25859.
[6] S. Saja, A. Bouazizi, B. Achiou, M. Ouammou, A. Albizane, J. Bennazha, S.A. Younssi, Elaboration and characterization of low-cost ceramic membrane made from natural Moroccan perlite for treatment of industrial wastewater, J. Environ. Chem. Eng. 6 (2018) 451–458. https://doi.org/10.1016/j.jece.2017.12.004.
[7] A. Belgada, B. Achiou, S. Alami Younssi, F.Z. Charik, M. Ouammou, J.A. Cody, R. Benhida, K. Khaless, Low-cost ceramic microfiltration membrane made from natural phosphate for pretreatment of raw seawater for desalination, J. Eur. Ceram. Soc. 41 (2021) 1613–1621. https://doi.org/10.1016/j.jeurceramsoc.2020.09.064.
[8] H. Ouaddari, A. Karim, B. Achiou, S. Saja, A. Aaddane, J. Bennazha, I. El Amrani El Hassani, M. Ouammou, A. Albizane, New low-cost ultrafiltration membrane made from purified natural clays for direct Red 80 dye removal, J. Environ. Chem. Eng. 7 (2019) 103268. https://doi.org/10.1016/j.jece.2019.103268.
[9] S. Benkhaya, B. Achiou, M. Ouammou, J. Bennazha, S. Alami Younssi, S. M'rabet, A. El Harfi, Preparation of low-cost composite membrane made of polysulfone/polyetherimide ultrafiltration layer and ceramic pozzolan support for dyes removal, Mater. Today Commun. 19 (2019) 212–219. https://doi.org/10.1016/j.mtcomm.2019.02.002.
[10] T. Arumugham, N.J. Kaleekkal, S. Gopal, J. Nambikkattu, R. K, A.M. Aboulella, S. Ranil Wickramasinghe, F. Banat, Recent developments in porous ceramic membranes for wastewater treatment and desalination: A review, J. Environ. Manage. 293 (2021) 112925. https://doi.org/10.1016/j.jenvman.2021.112925.
[11] C. Algieri, E. Drioli, Zeolite membranes: Synthesis and applications, Sep. Purif. Technol. 278 (2021) 119295. https://doi.org/10.1016/j.seppur.2021.119295.

[12] L. Wang, J. Yang, W. Raza, J. Wang, J. Lu, Y. Zhang, G. He, Sustainable fabrication of large-scale tubular LTA zeolite membranes by a simple wet gel conversion, Microporous Mesoporous Mater. 329 (2022) 111541. https://doi.org/10.1016/j.micromeso.2021.111541.
[13] F.Z. Charik, B. Achiou, A. Belgada, M. Ouammou, S. Alami Younssi, Zeolite materials in service of membrane technology, in: A. Mahler (Ed.), Zeolites Adv. Res. Appl., Nova Science, 2020: pp. 133–162.
[14] W. Raza, J. Wang, J. Yang, T. Tsuru, Progress in pervaporation membranes for dehydration of acetic acid, Sep. Purif. Technol. 262 (2021) 118338. https://doi.org/10.1016/j.seppur.2021.118338.
[15] B. Achiou, D. Beqqour, H. Elomari, A. Bouazizi, M. Ouammou, M. Bouhria, A. Aaddane, K. Khiat, S. Alami Younssi, Preparation of inexpensive NaA zeolite membrane on pozzolan support at low temperature for dehydration of alcohol solutions, J. Environ. Chem. Eng. 6 (2018) 4429–4437. https://doi.org/10.1016/j.jece.2018.06.049.
[16] B. Liu, H. Kita, K. Yogo, Preparation of Si-rich LTA zeolite membrane using organic template-free solution for methanol dehydration, Sep. Purif. Technol. 239 (2020) 116533. https://doi.org/10.1016/j.seppur.2020.116533.
[17] S.M. Lee, N. Xu, J.R. Grace, A. Li, C.J. Lim, S.S. Kim, F. Fotovat, A. Schaadt, R.J. White, Structure, stability and permeation properties of NaA zeolite membranes for H2O/H2 and CH3OH/H2 separations, J. Eur. Ceram. Soc. 38 (2018) 211–219. https://doi.org/10.1016/j.jeurceramsoc.2017.08.012.
[18] M. Mirfendereski, T. Mohammadi, Effects of Synthesis Parameters on the Characteristics of Naa Type Zeolite Nanoparticles, in: 2016. https://doi.org/10.11159/icnnfc16.113.
[19] Y. Cao, Y.-X. Li, M. Wang, Z.-L. Xu, Y.-M. Wei, B.-J. Shen, K.-K. Zhu, High-flux NaA zeolite pervaporation membranes dynamically synthesized on the alumina hollow fiber inner-surface in a continuous flow system, J. Membr. Sci. 570–571 (2019) 445–454. https://doi.org/10.1016/j.memsci.2018.10.043.
[20] M.P. Moisés, C.T.P. da Silva, J.G. Meneguin, E.M. Girotto, E. Radovanovic, Synthesis of zeolite NaA from sugarcane bagasse ash, Mater. Lett. 108 (2013) 243–246. https://doi.org/10.1016/j.matlet.2013.06.086.
[21] A.R. Loiola, J.C.R.A. Andrade, J.M. Sasaki, L.R.D. da Silva, Structural analysis of zeolite NaA synthesized by a cost-effective hydrothermal method using kaolin and its use as water softener, J. Colloid Interface Sci. 367 (2012) 34–39. https://doi.org/10.1016/j.jcis.2010.11.026.
[22] J. Madhu, V. Madurai Ramakrishnan, P. Palanichamy, A. Santhanam, M. Natarajan, P. Ponnaian, K. Brindhadevi, A. Pugazhendhi, D. Velauthapillai, Rubik's cube shaped organic template free hydrothermal synthesis and characterization of zeolite NaA for CO2 adsorption, Fuel. 317 (2022) 123492. https://doi.org/10.1016/j.fuel.2022.123492.
[23] F. Hasan, R. Singh, G. Li, D. Zhao, P.A. Webley, Direct synthesis of hierarchical LTA zeolite via a low crystallization and growth rate technique in presence of cetyltrimethylammonium bromide, J. Colloid Interface Sci. 382 (2012) 1–12. https://doi.org/10.1016/j.jcis.2012.05.027.
[24] S. Shirazian, S.N. Ashrafizadeh, Synthesis of substrate-modified LTA zeolite membranes for dehydration of natural gas, Fuel. 148 (2015) 112–119. https://doi.org/10.1016/j.fuel.2015.01.086.
[25] X. Wu, Z. Yan, Y. Li, B. Zhu, T. Gui, Y. Li, M. Zhu, F. Zhang, X. Chen, H. Kita, Fabrication of low cost and high performance NaA zeolite membranes on 100-cm-long coarse macroporous supports for pervaporation dehydration of dimethoxymethane, Sep. Purif. Technol. 281 (2022) 119877. https://doi.org/10.1016/j.seppur.2021.119877.

[26] C. Yu, C. Zhong, Y. Liu, X. Gu, G. Yang, W. Xing, N. Xu, Pervaporation dehydration of ethylene glycol by NaA zeolite membranes, Chem. Eng. Res. Des. 90 (2012) 1372–1380. https://doi.org/10.1016/j.cherd.2011.12.003.
[27] M. Jafari, A. Bayat, T. Mohammadi, M. Kazemimoghadam, Dehydration of ethylene glycol by pervaporation using gamma alumina/NaA zeolite composite membrane, Chem. Eng. Res. Des. 91 (2013) 2412–2419. https://doi.org/10.1016/j.cherd.2013.04.016.
[28] D. Liu, Y. Zhang, J. Jiang, X. Wang, C. Zhang, X. Gu, High-performance NaA zeolite membranes supported on four-channel ceramic hollow fibers for ethanol dehydration, RSC Adv. 5 (2015) 95866–95871. https://doi.org/10.1039/C5RA18711G.
[29] Y. Zhang, X. Zhu, S. Chen, J. Liu, Z. Hong, J. Wang, Z. Li, X. Gao, R. Xu, X. Gu, TiO2-decorated NaA zeolite membranes with improved separation stability for pervaporation dehydration of N, N-Dimethylacetamide, J. Membr. Sci. 634 (2021) 119398. https://doi.org/10.1016/j.memsci.2021.119398.
[30] Z. Huang, X. Ru, Y.-T. Zhu, Y. Guo, L. Teng, Poly(vinyl alcohol)/ZSM-5 zeolite mixed matrix membranes for pervaporation dehydration of isopropanol/water solution through response surface methodology, Chem. Eng. Res. Des. 144 (2019) 19–34. https://doi.org/10.1016/j.cherd.2019.01.026.
[31] F. Qu, R. Shi, L. Peng, Y. Zhang, X. Gu, X. Wang, S. Murad, Understanding the effect of zeolite crystal expansion/contraction on separation performance of NaA zeolite membrane: A combined experimental and molecular simulation study, J. Membr. Sci. 539 (2017) 14–23. https://doi.org/10.1016/j.memsci.2017.05.057.
[32] K.V.V. Satyannarayana, S.L. Sandhya Rani, S. Baranidharan, R.V. Kumar, Indigenous bentonite based tubular ceramic microfiltration membrane: Elaboration, characterization, and evaluation of environmental impacts using life cycle techniques, Ceram. Int. (2022) S0272884222009488. https://doi.org/10.1016/j.ceramint.2022.03.156.
[33] I.G. Wenten, P.T. Dharmawijaya, P.T.P. Aryanti, R.R. Mukti, K. Khoiruddin, LTA zeolite membranes: current progress and challenges in pervaporation, RSC Adv. 7 (2017) 29520–29539. https://doi.org/10.1039/C7RA03341A.
[34] S. Emani, R. Uppaluri, M.K. Purkait, Preparation and characterization of low cost ceramic membranes for mosambi juice clarification, Desalination. 317 (2013) 32–40. https://doi.org/10.1016/j.desal.2013.02.024.
[35] A. Dhivya, A. Keshav, Fabrication of ball clay based low-cost ceramic membrane supports and their characterization for microfiltration application, J. Indian Chem. Soc. 99 (2022) 100557. https://doi.org/10.1016/j.jics.2022.100557.
[36] B.K. Nandi, R. Uppaluri, M.K. Purkait, Preparation and characterization of low cost ceramic membranes for micro-filtration applications, Appl. Clay Sci. 42 (2008) 102–110. https://doi.org/10.1016/j.clay.2007.12.001.

Table 1

Estimation cost of kaolinite support and NaA zeolite layer.

	Kaolinite support		Zeolite layer	
	Material	**Cost of support ($ m^{-2})**	**Materials**	**Cost of the zeolite layer ($ m^{-2})**
Raw materials	Kaolinite	11.54	Sodium hydroxide	4.09
			Sodium aluminate	0.56
			Sodium silicate	86.07
Energy cost	**Equipment**	**Cost of energy ($ m^{-2})**	**Equipment**	**Cost of energy ($ m^{-2})**
	Grinder	0.0200	Oven	0.19
	Sifter	0.0007		
	Furnace	7.0700		
	Total cost of support ($ m^{-2})	18.63	**Total cost of zeolite layer ($ m^{-2})**	90.91

Table 2

Comparison of preparation cost of clay-based membranes.

Membrane	Configuration	Estimated cost ($ m^{-2})	Reference
Kaolin, quartz, sodium metasilicate, sodium carbonate, calcium carbonate, boric acid and polyvinyl alcohol	Disc	78	**[34]**
Ball clay, quartz and calcium carbonate	Disc	17.07	**[35]**
Kaolin, quartz, sodium carbonate, feldspar, boric acid, sodium metasilicate and sodium carbonate	Disc	130	**[36]**
Kaolinite	Disc	18.63	This work

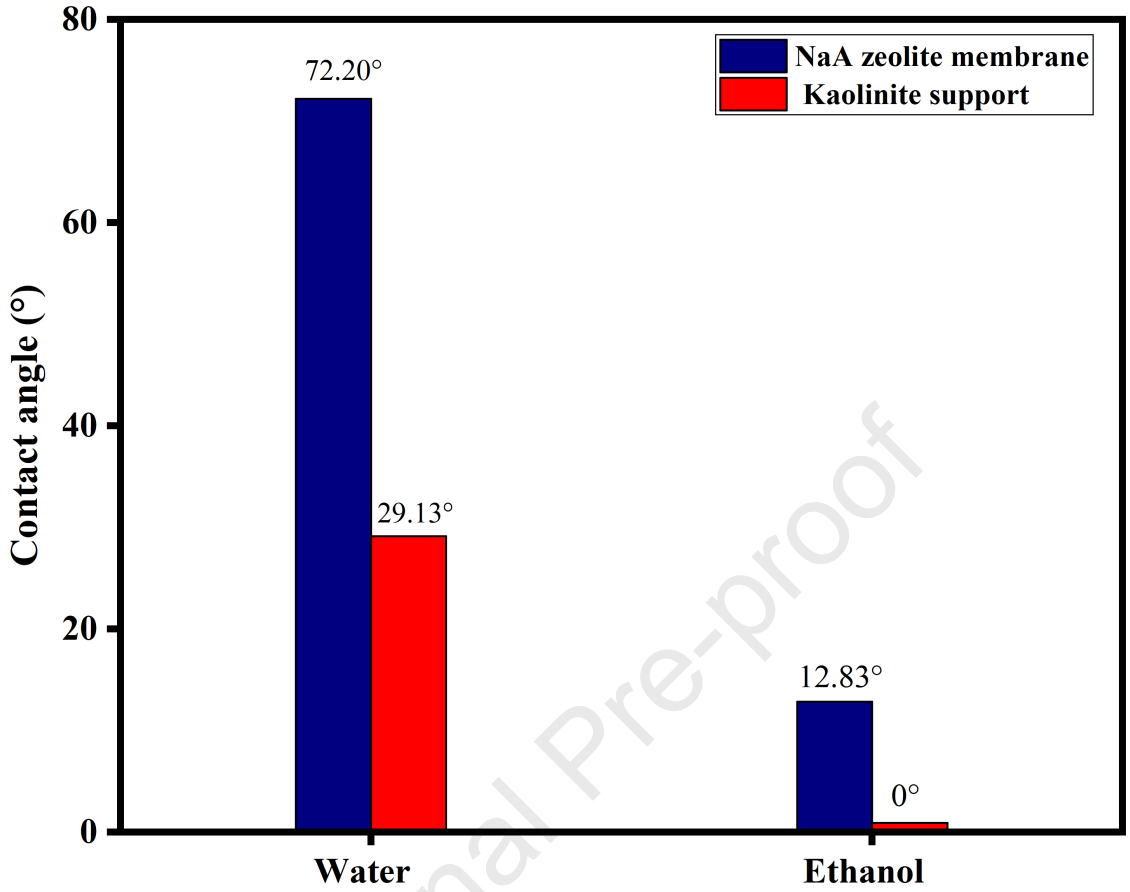

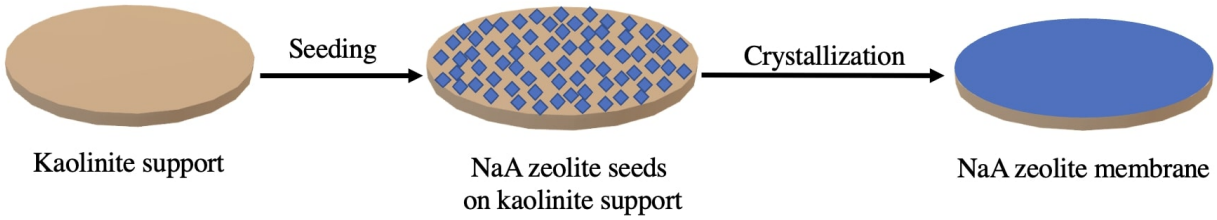

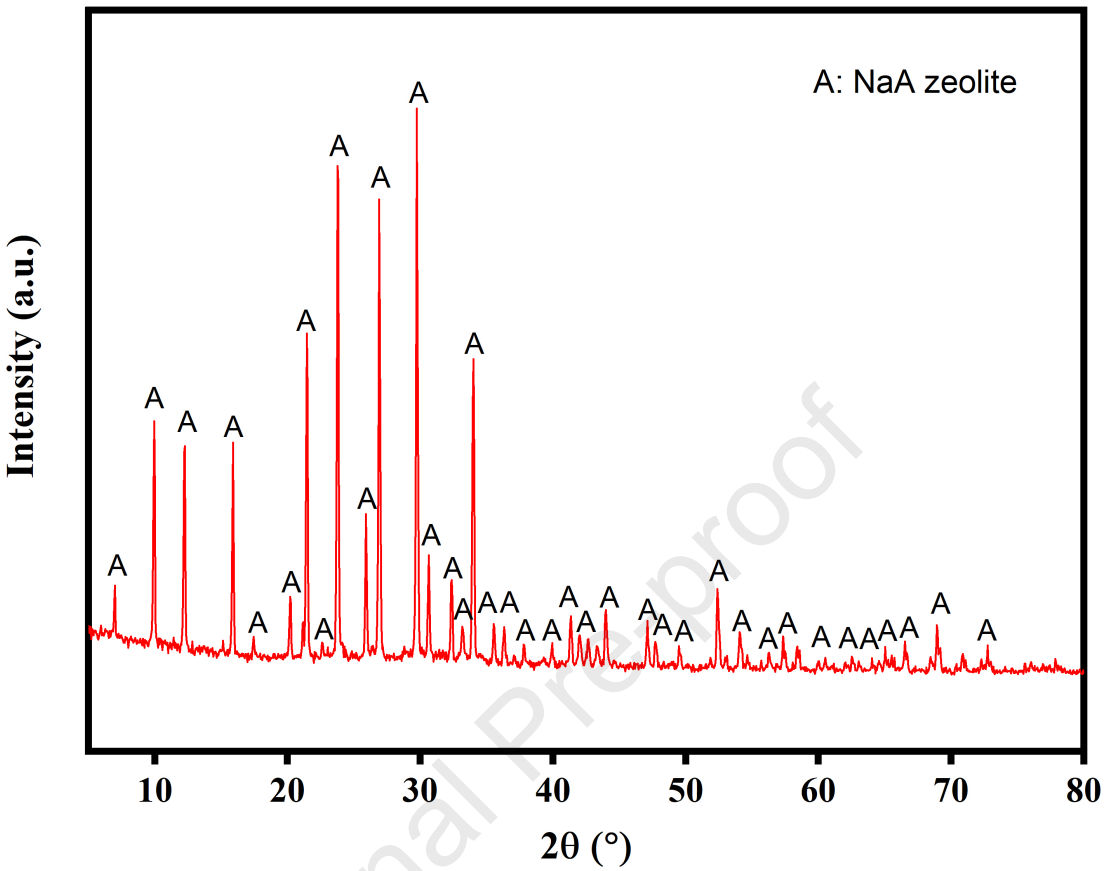

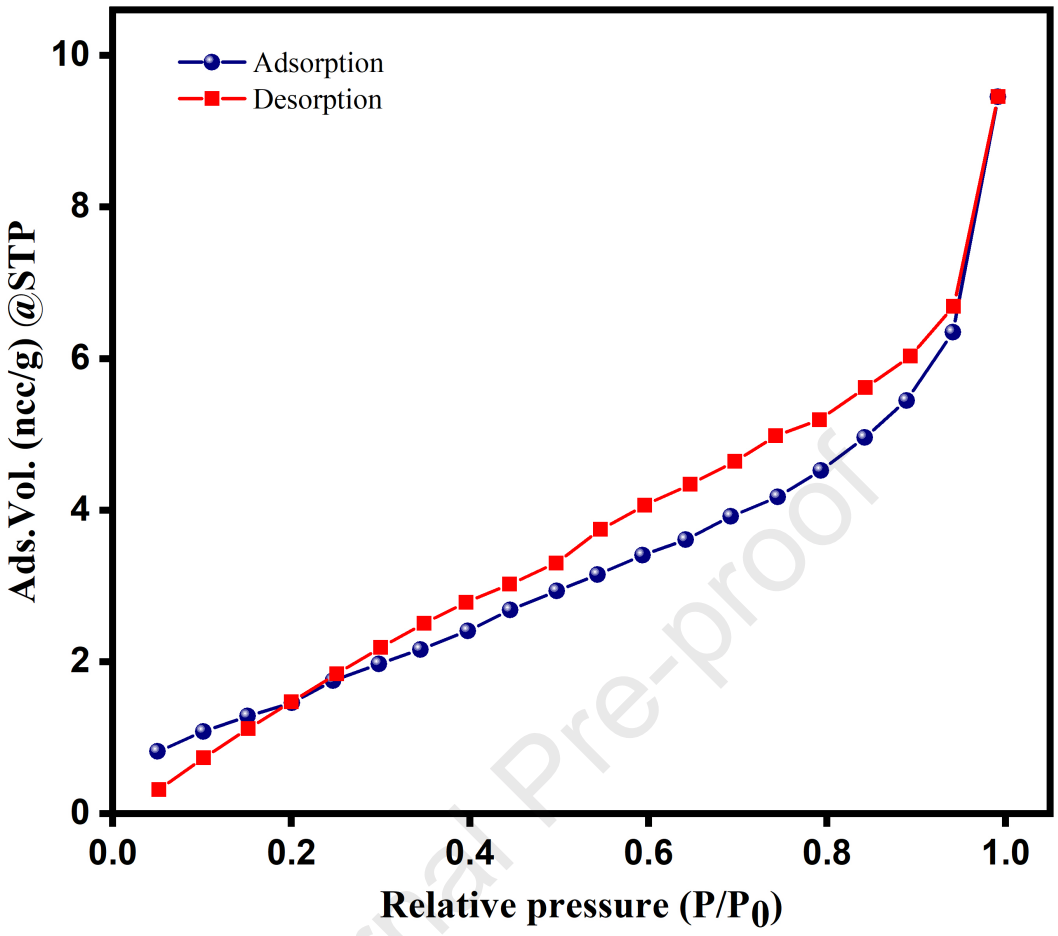

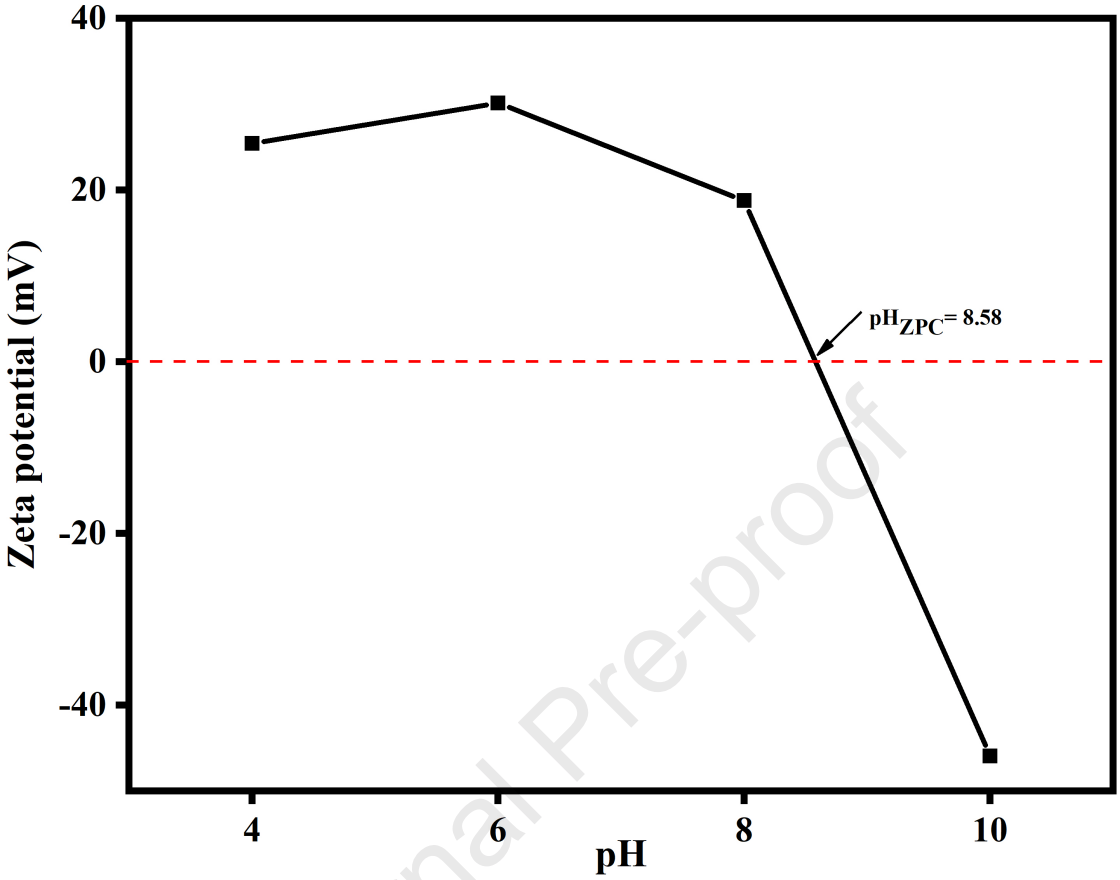

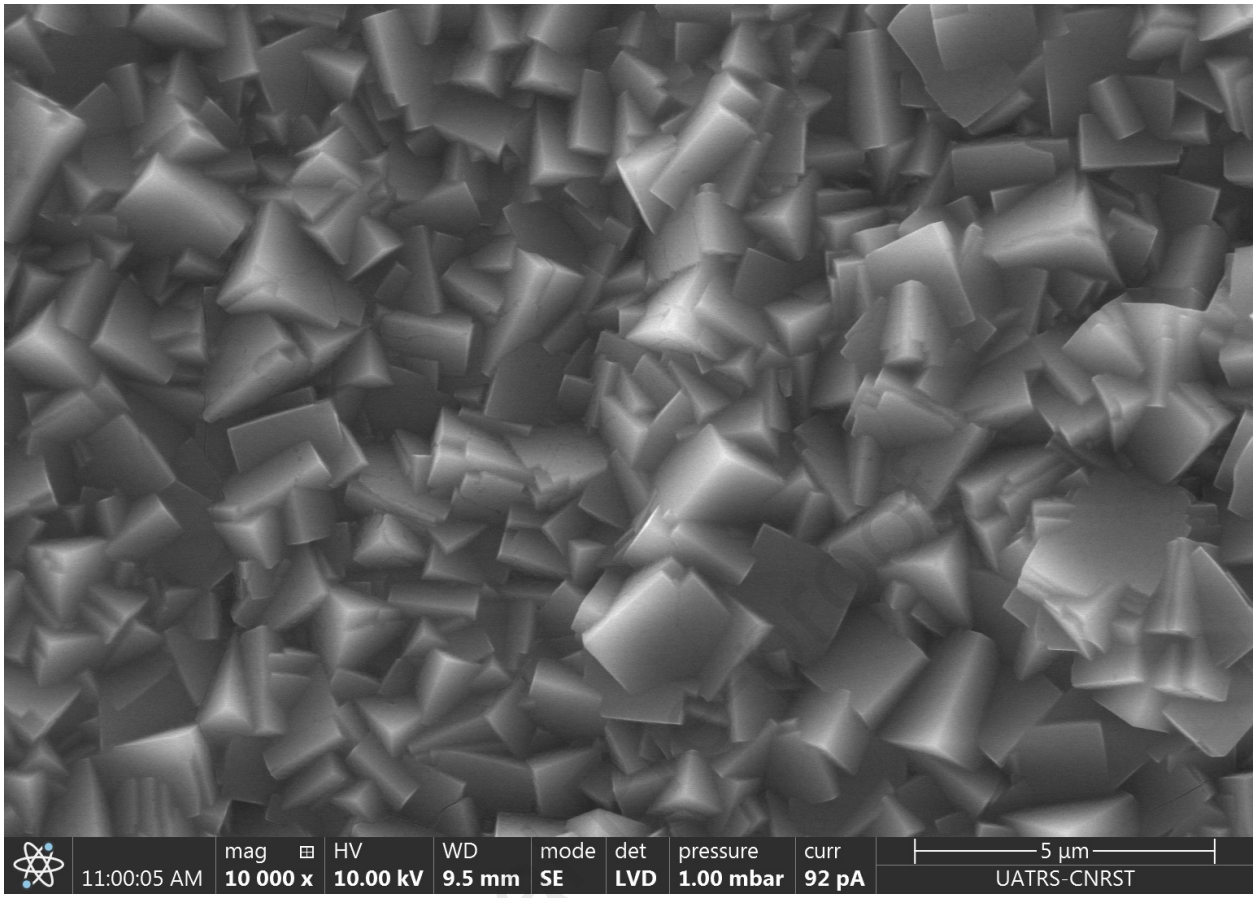
11:00:05 AM
mag
10 000 x
HV
10.00 kV
WD
9.5 mm
mode
SE
det
LVD
pressure
1.00 mbar
curr
92 pA
5 µm
UATRS-CNRST

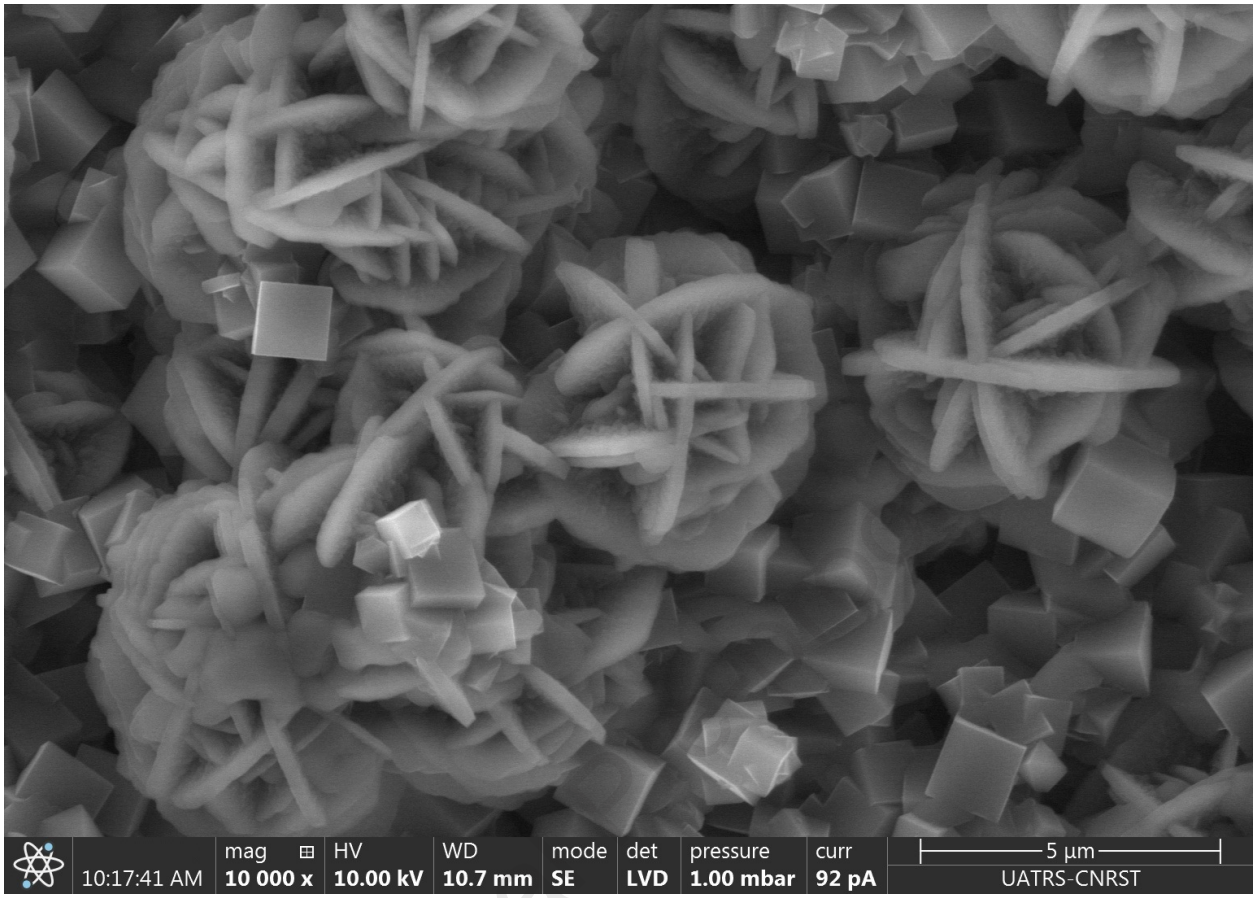
10:17:41 AM
mag
10 000 x
HV
10.00 kV
WD
10.7 mm
mode
SE
det
LVD
pressure
1.00 mbar
curr
92 pA
5 µm
UATRS-CNRST

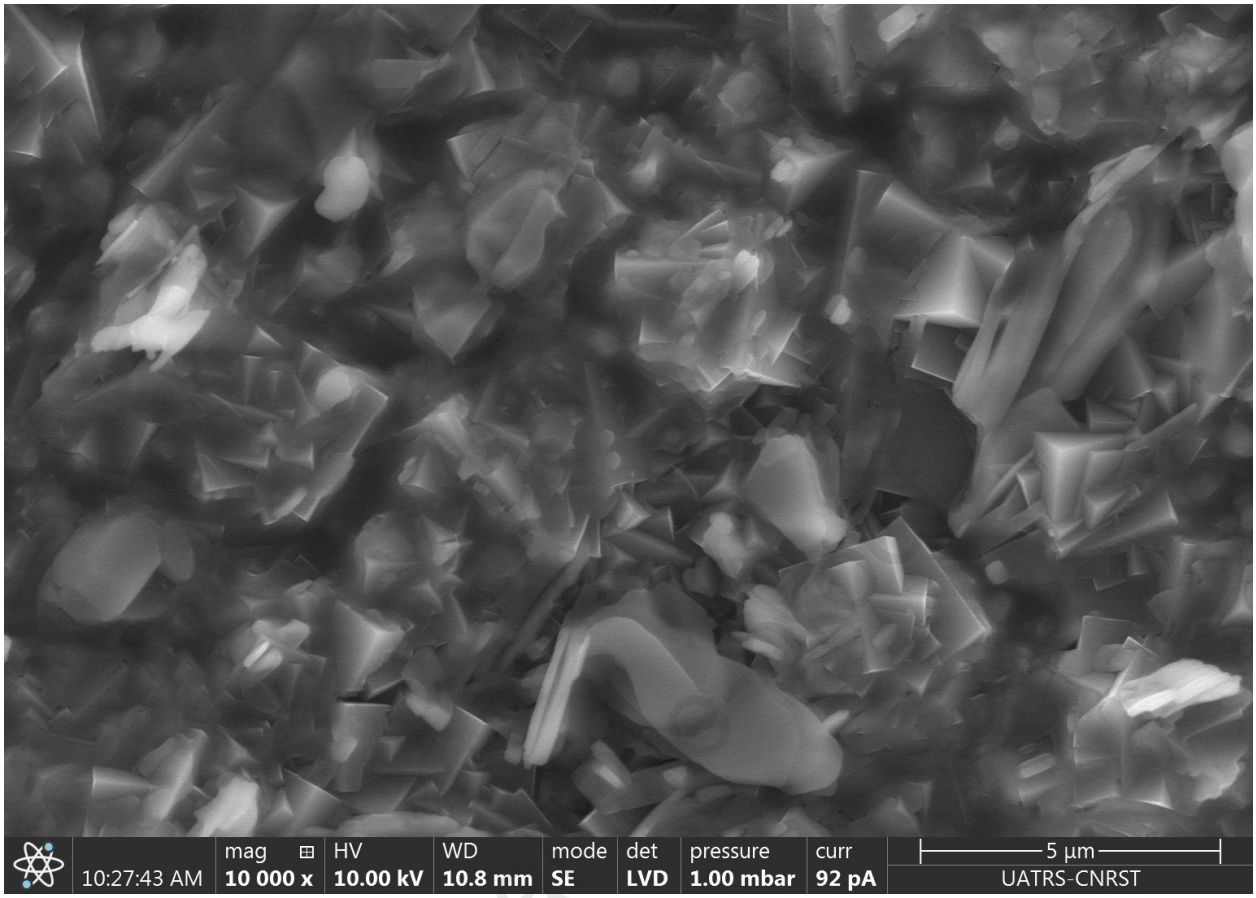
10:27:43 AM
mag
10 000 x
HV
10.00 kV
WD
10.8 mm
mode
SE
det
LVD
pressure
1.00 mbar
curr
92 pA
5 µm
UATRS-CNRST

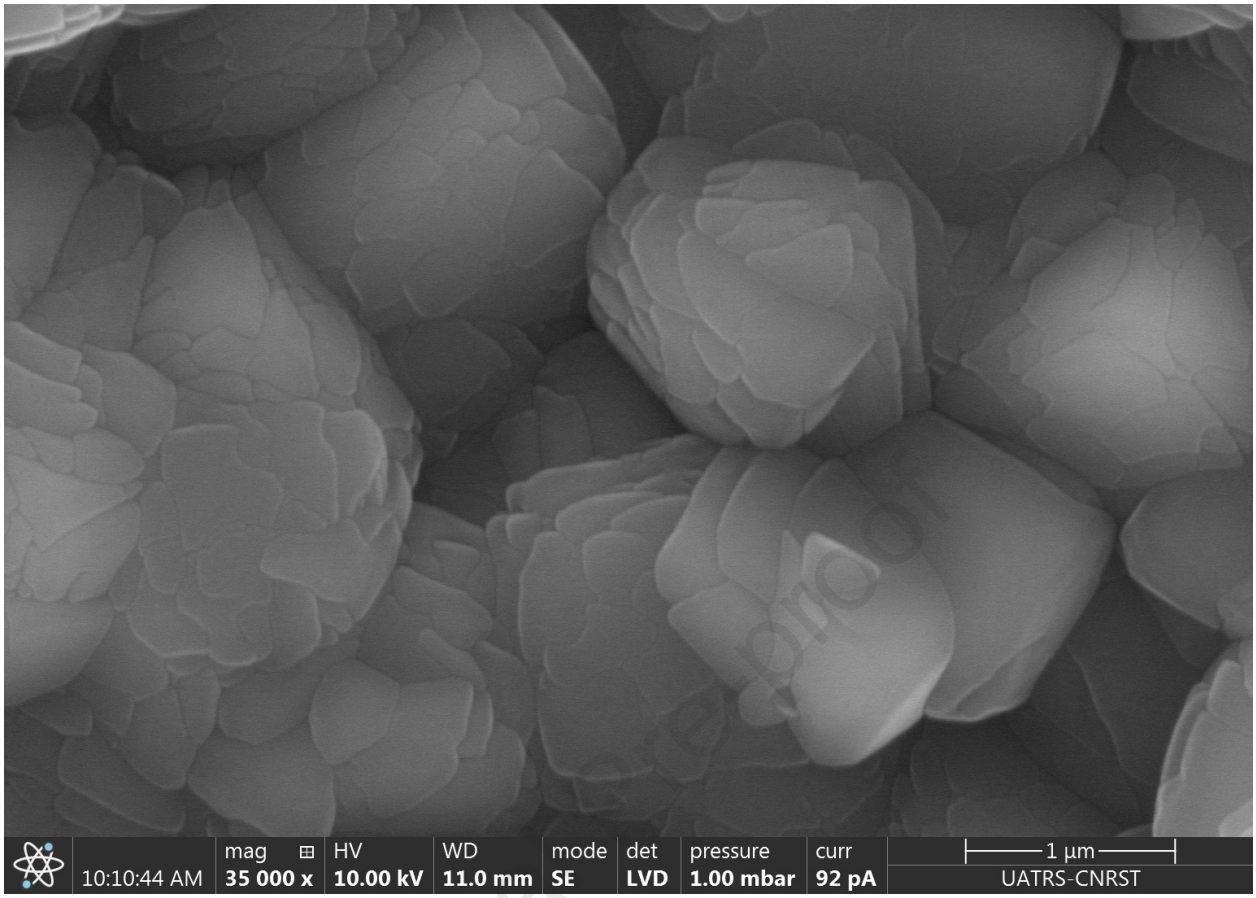

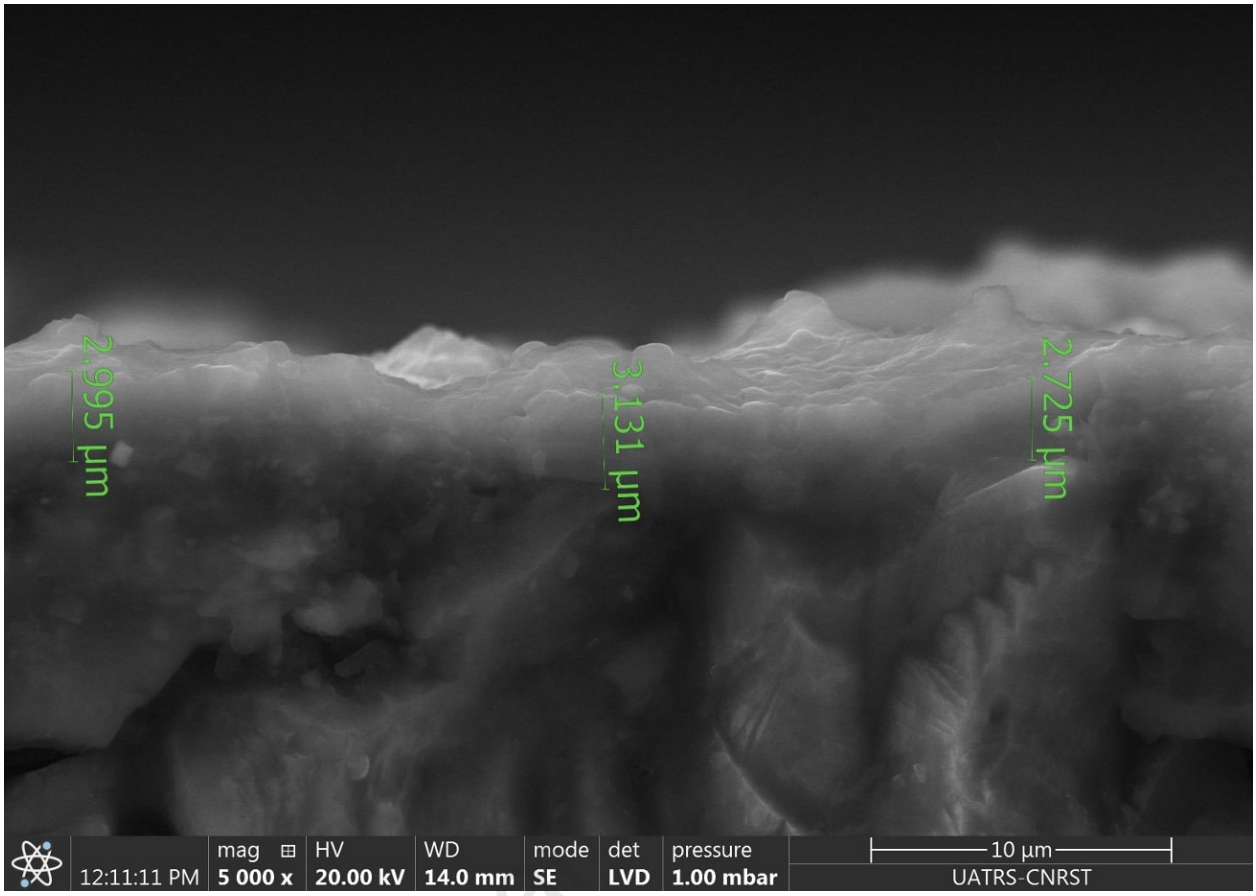
2.995 µm
3.131 µm
2.725 µm
12:11:11 PM
mag
5 000 x
HV
20.00 kV
WD
14.0 mm
mode
SE
det
LVD
pressure
1.00 mbar
10 µm
UATRS-CNRST

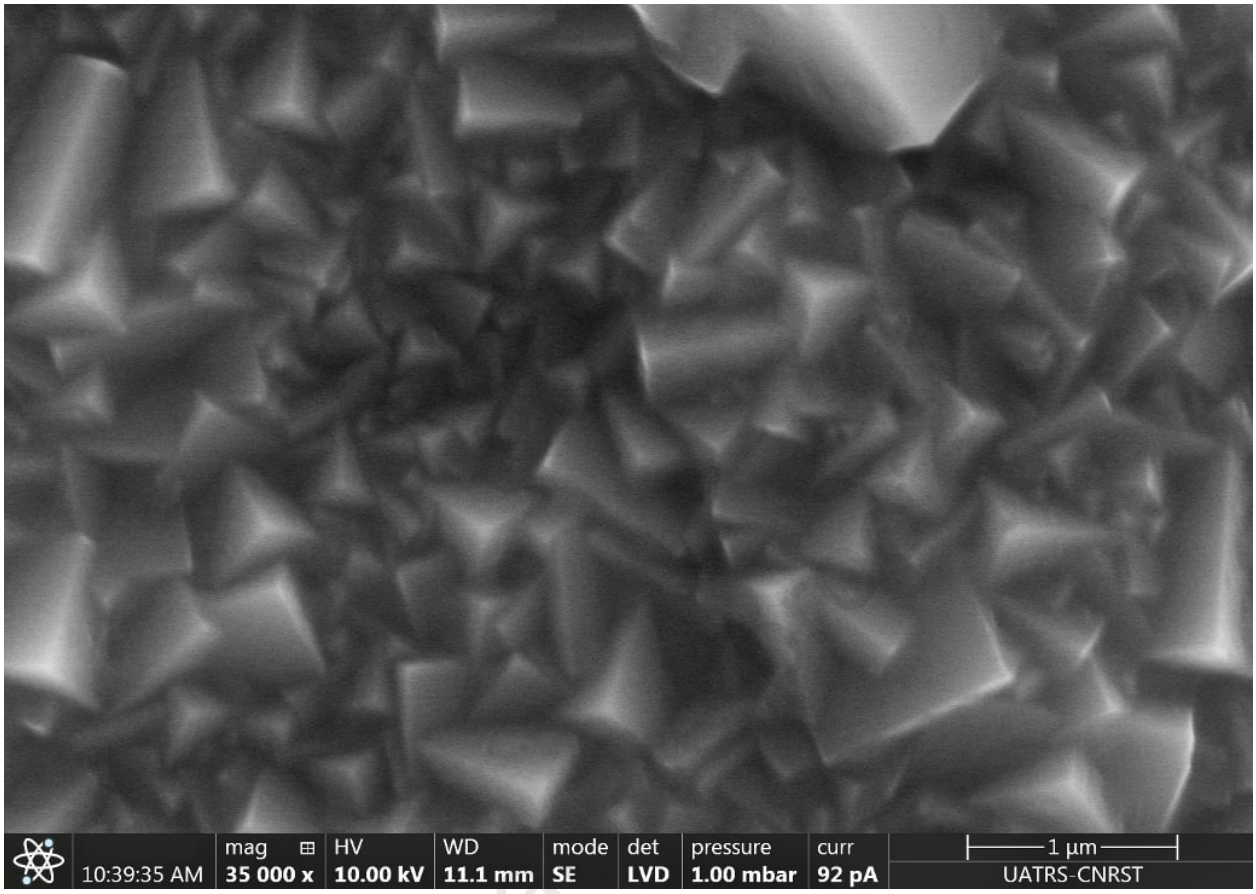
10:39:35 AM
mag
35 000 x
HV
10.00 kV
WD
11.1 mm
mode
SE
det
LVD
pressure
1.00 mbar
curr
92 pA
1 µm
UATRS-CNRST

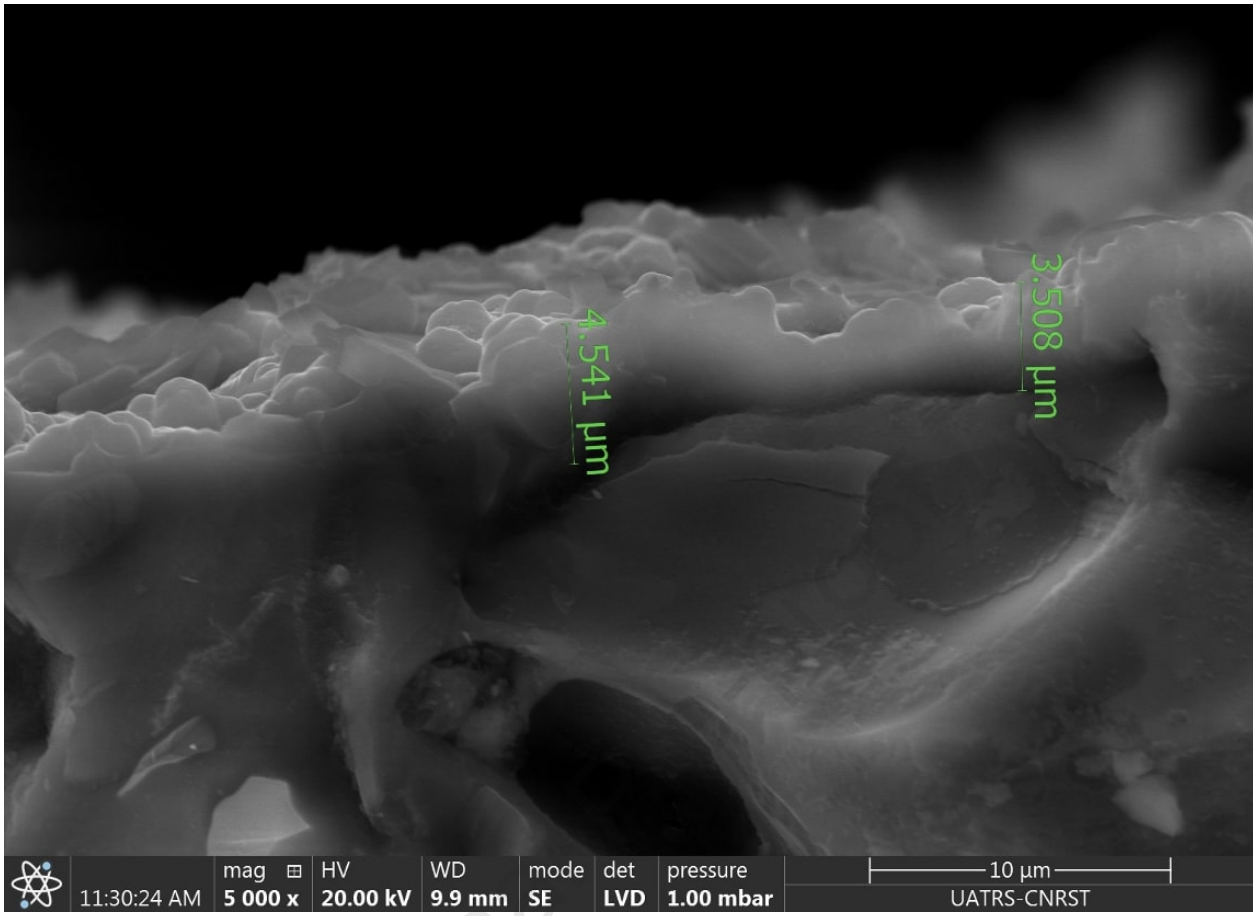
4.541 µm
3.508 µm
11:30:24 AM
mag
5 000 x
HV
20.00 kV
WD
9.9 mm
mode
SE
det
LVD
pressure
1.00 mbar
10 µm
UATRS-CNRST

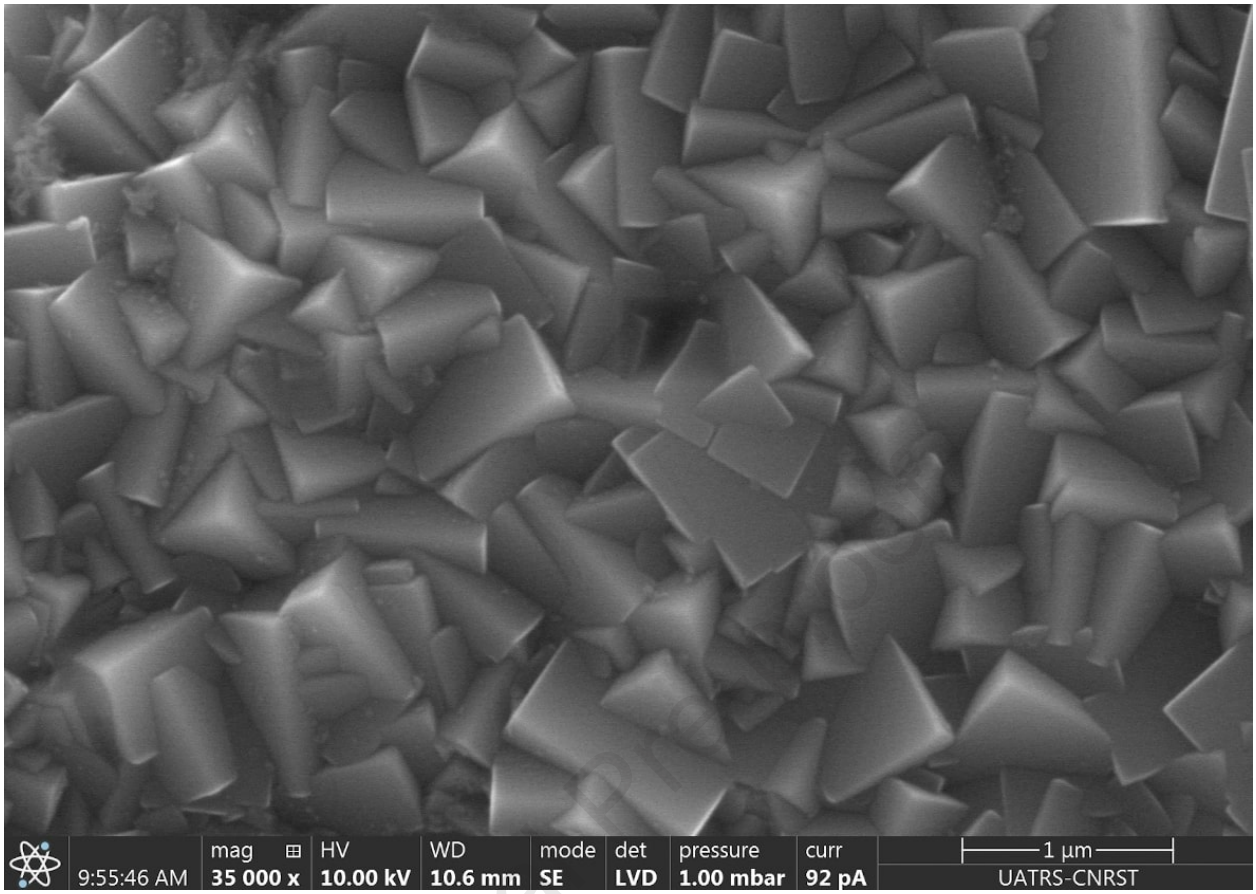

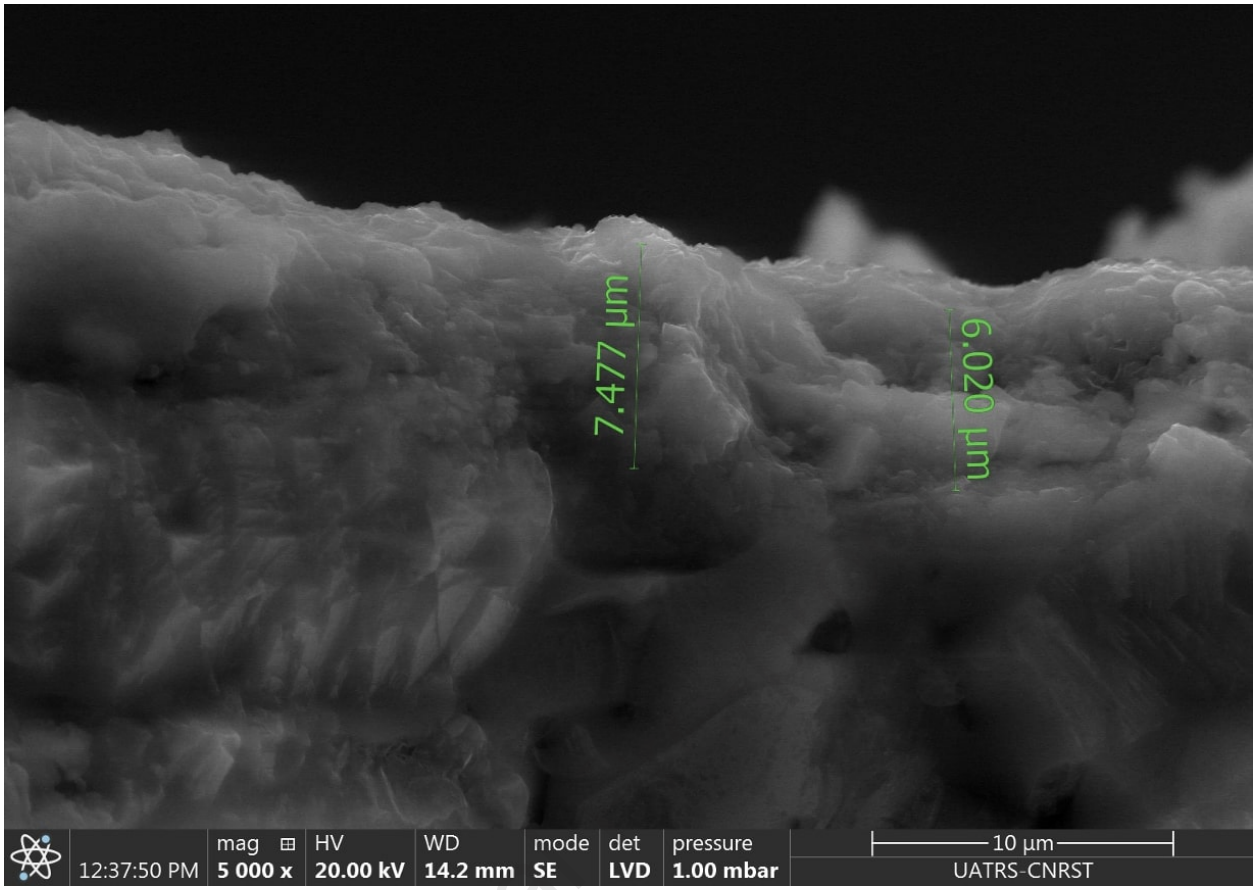
7.477 µm
6.020 µm
12:37:50 PM
mag
5 000 x
HV
20.00 kV
WD
14.2 mm
mode
SE
det
LVD
pressure
1.00 mbar
10 µm
UATRS-CNRST

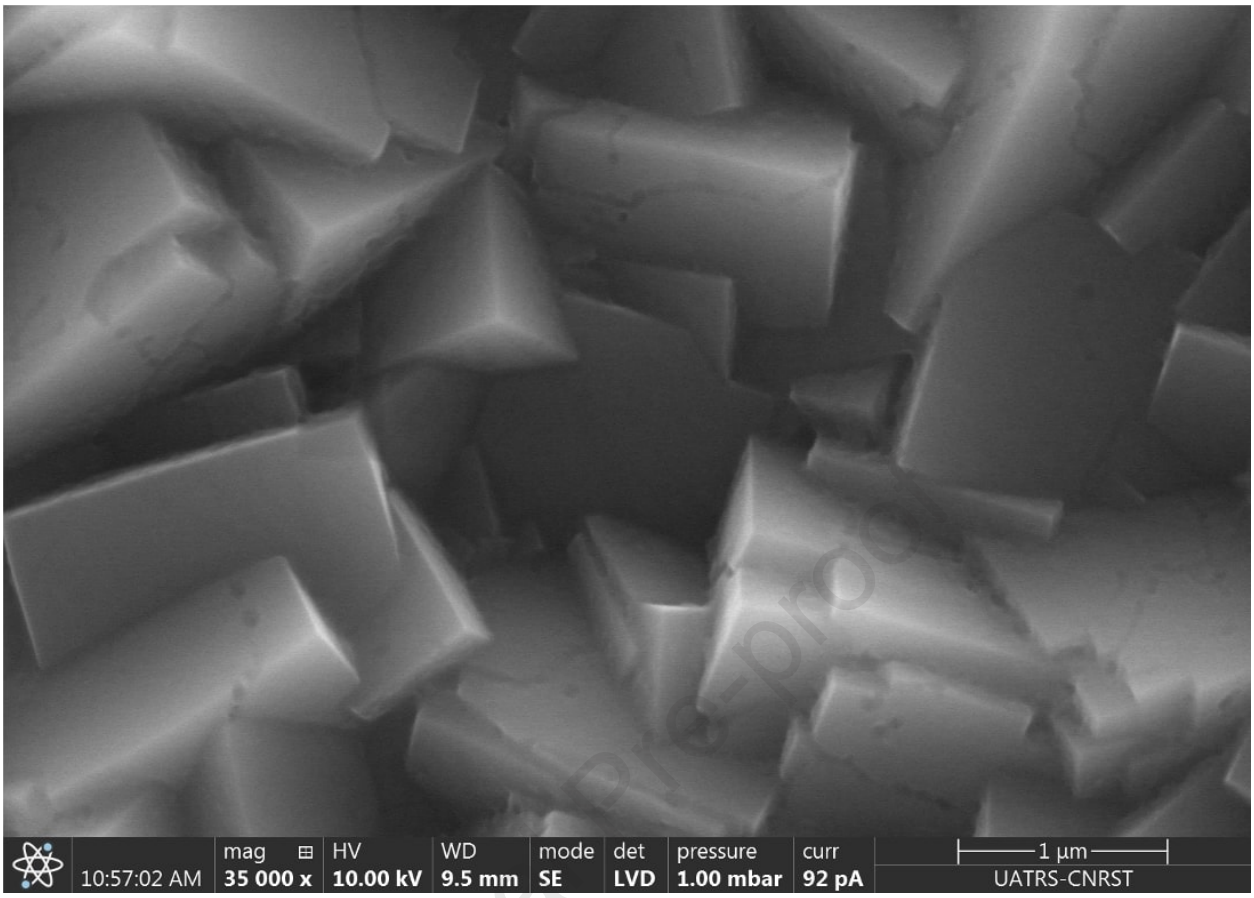

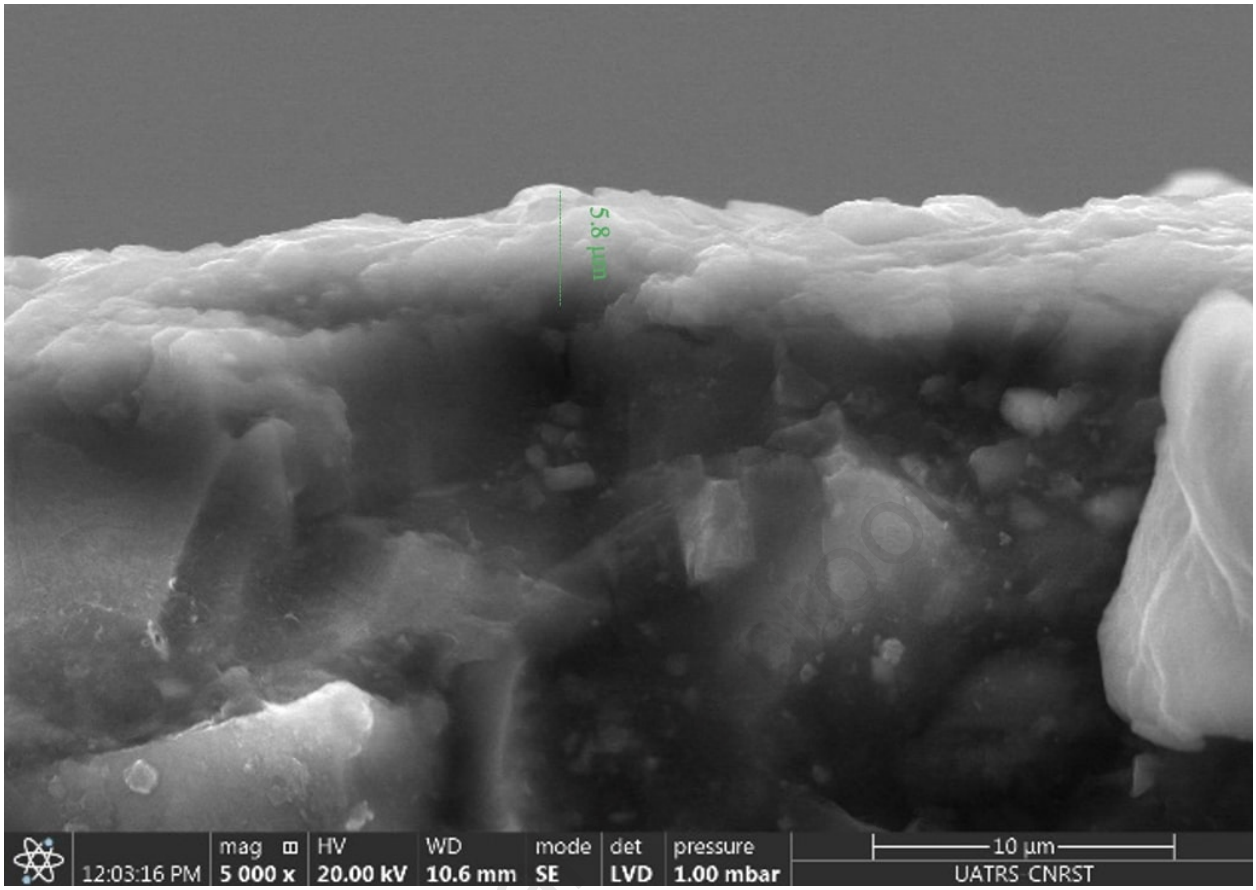

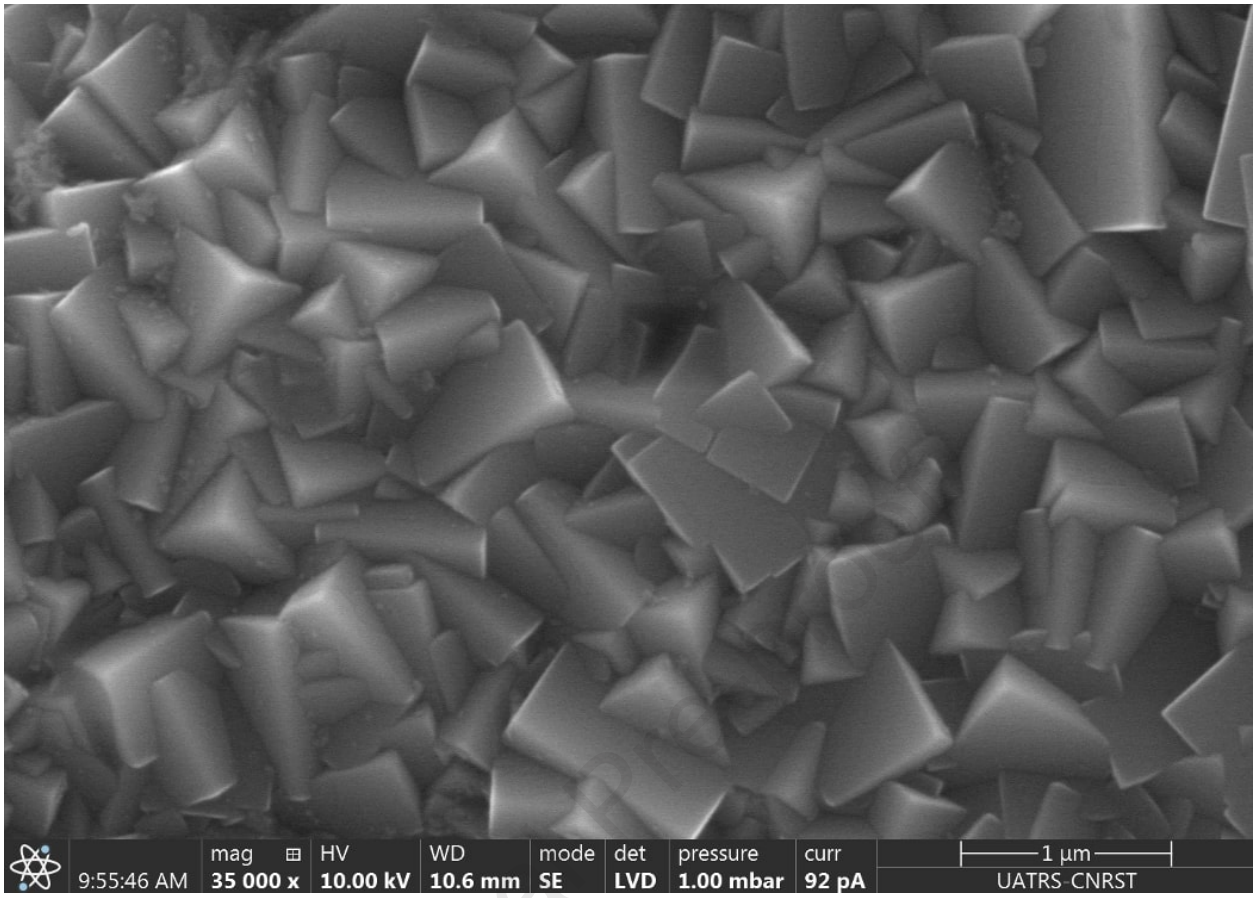

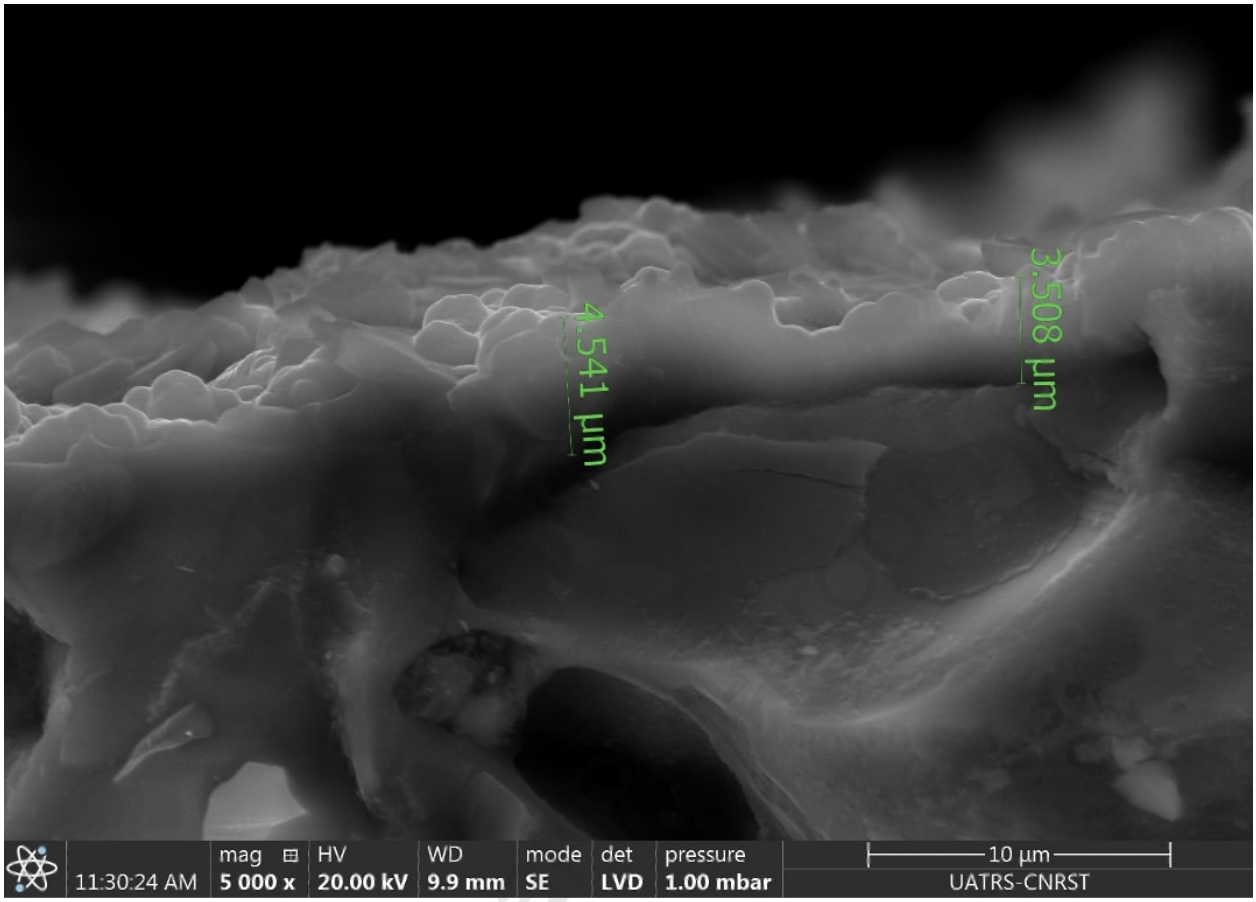
4.541 µm
3.508 µm
11:30:24 AM
mag
5 000 x
HV
20.00 kV
WD
9.9 mm
mode
SE
det
LVD
pressure
1.00 mbar
10 µm
UATRS-CNRST

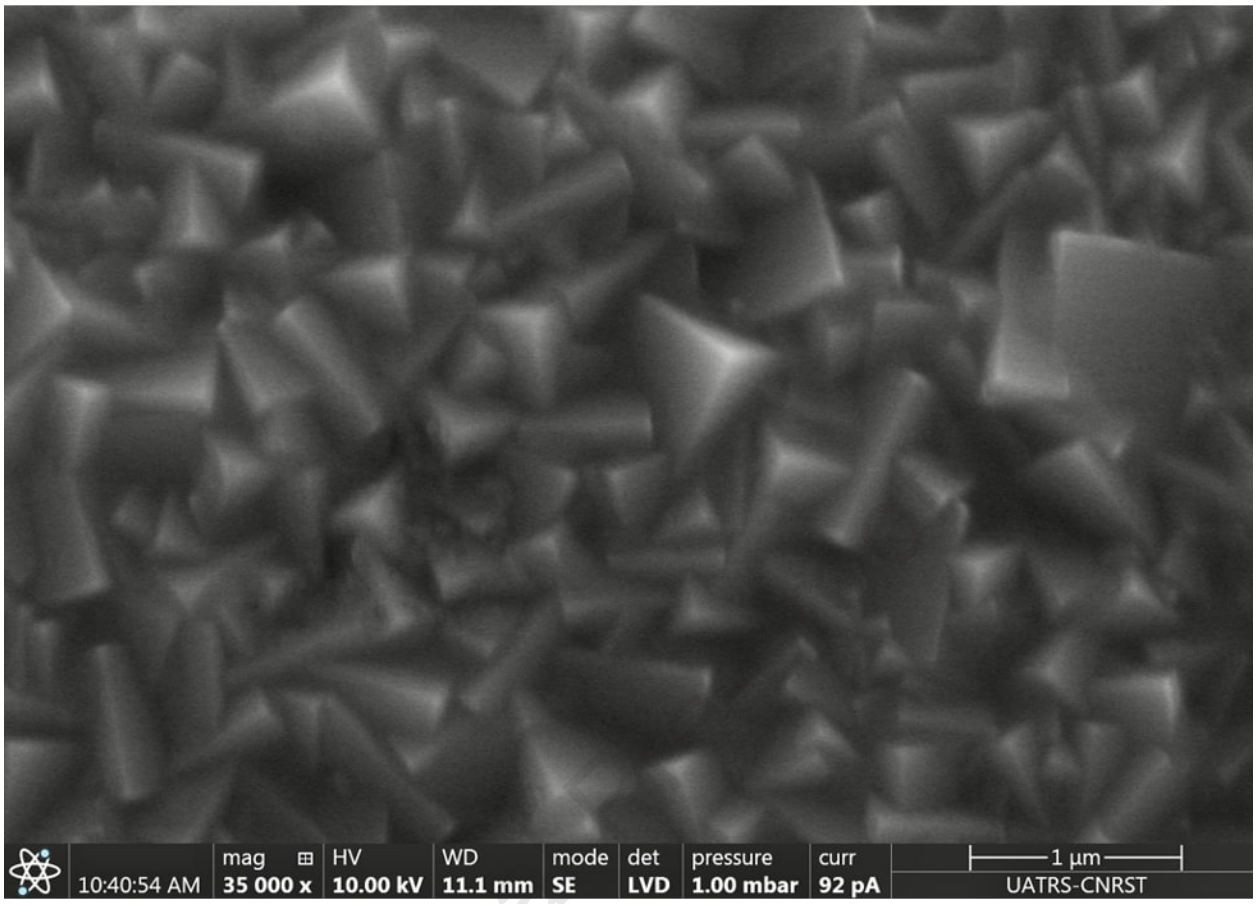
10:40:54 AM
mag
35 000 x
HV
10.00 kV
WD
11.1 mm
mode
SE
det
LVD
pressure
1.00 mbar
curr
92 pA
1 µm
UATRS-CNRST

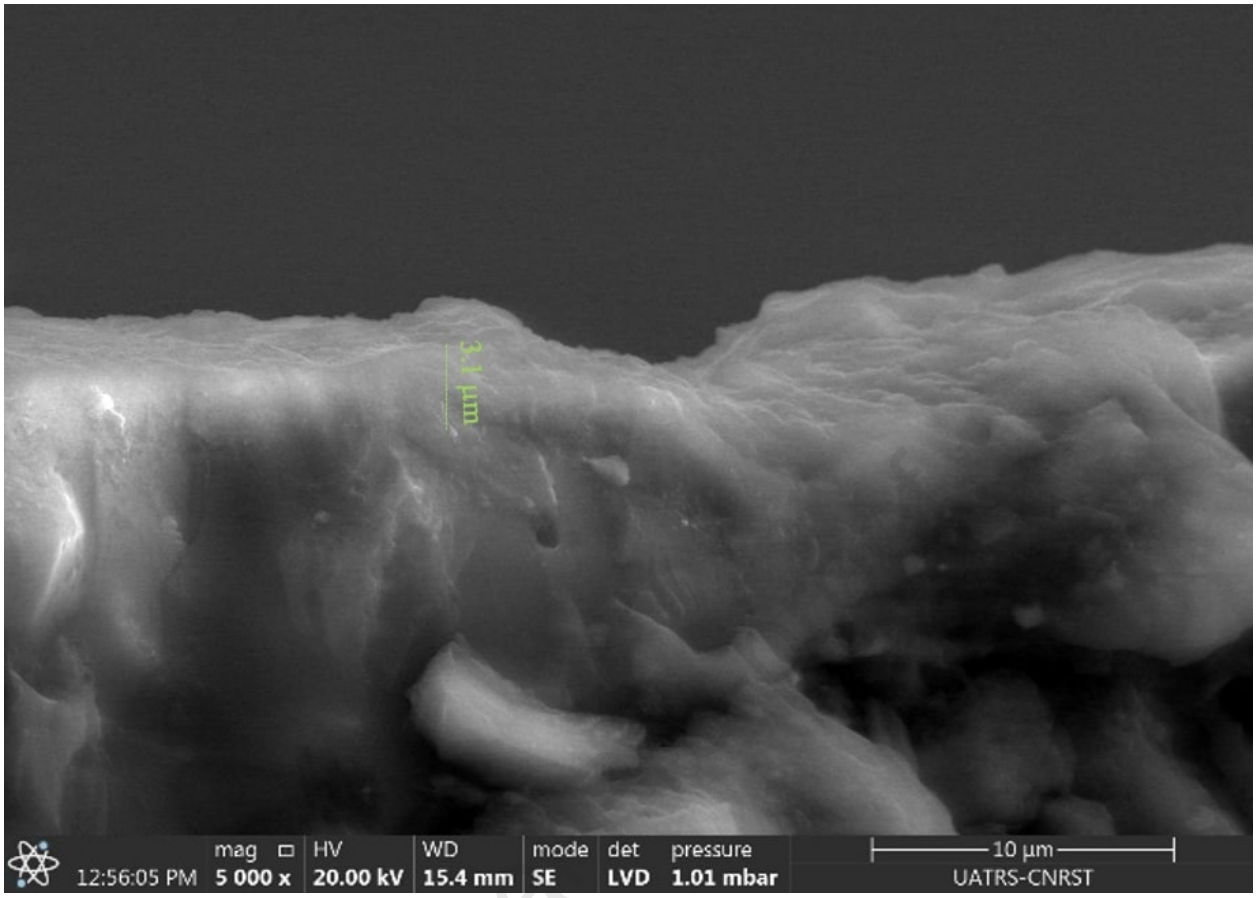
3.1 µm
mag
5 000 x
HV
20.00 kV
WD
15.4 mm
mode
SE
det
LVD
pressure
1.01 mbar
12:56:05 PM
10 µm
UATRS-CNRST

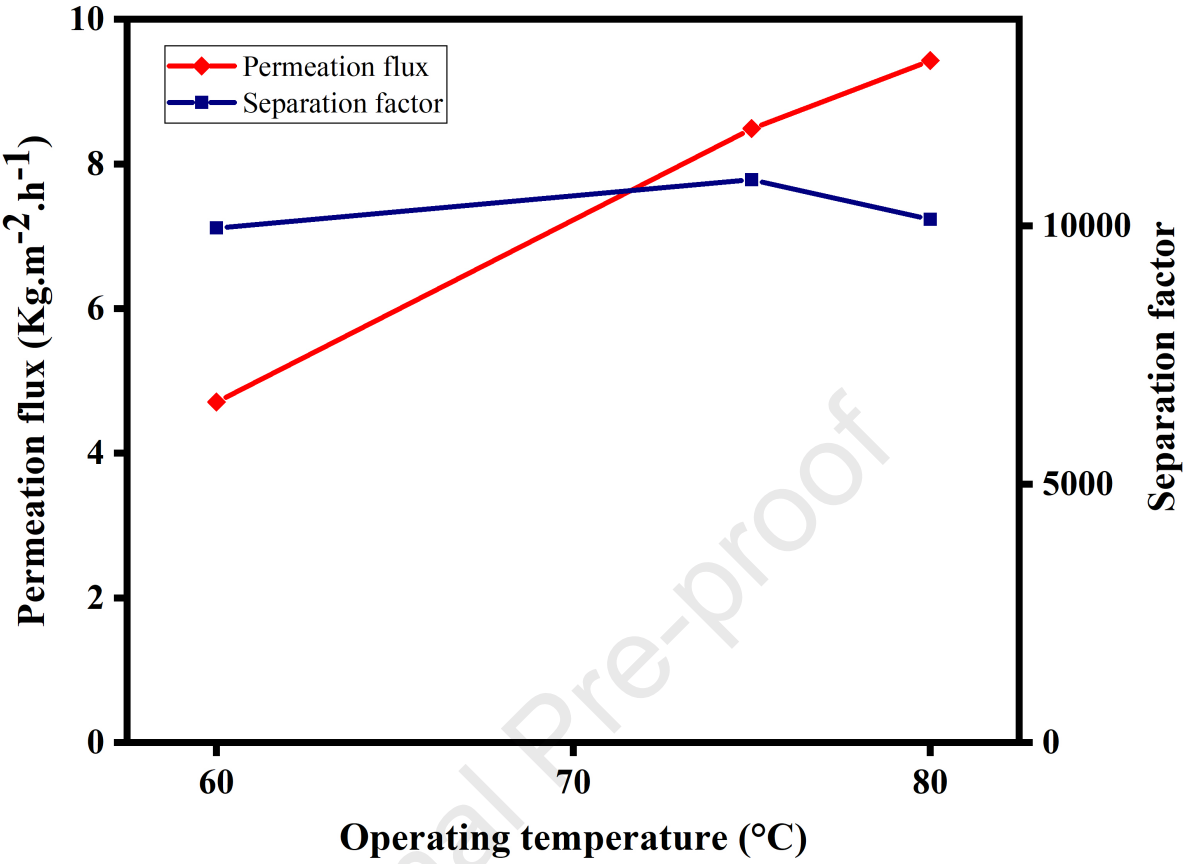

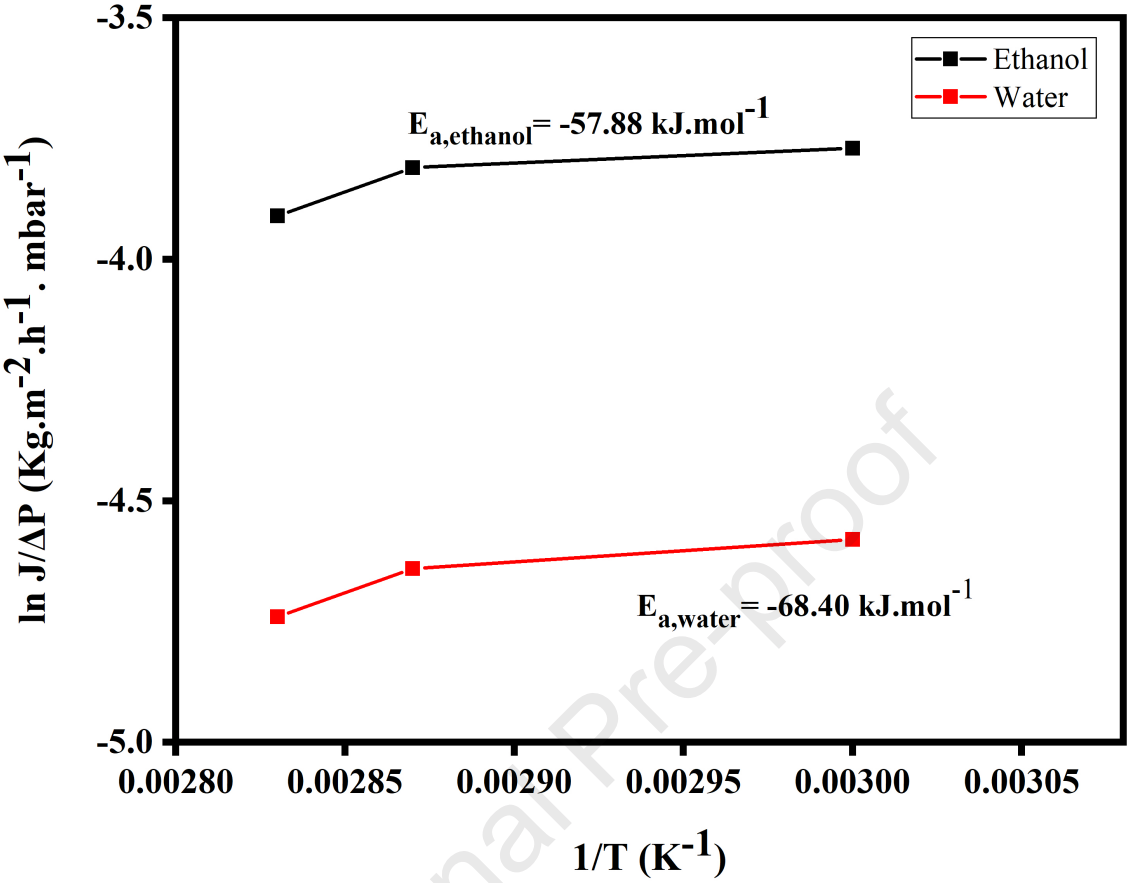

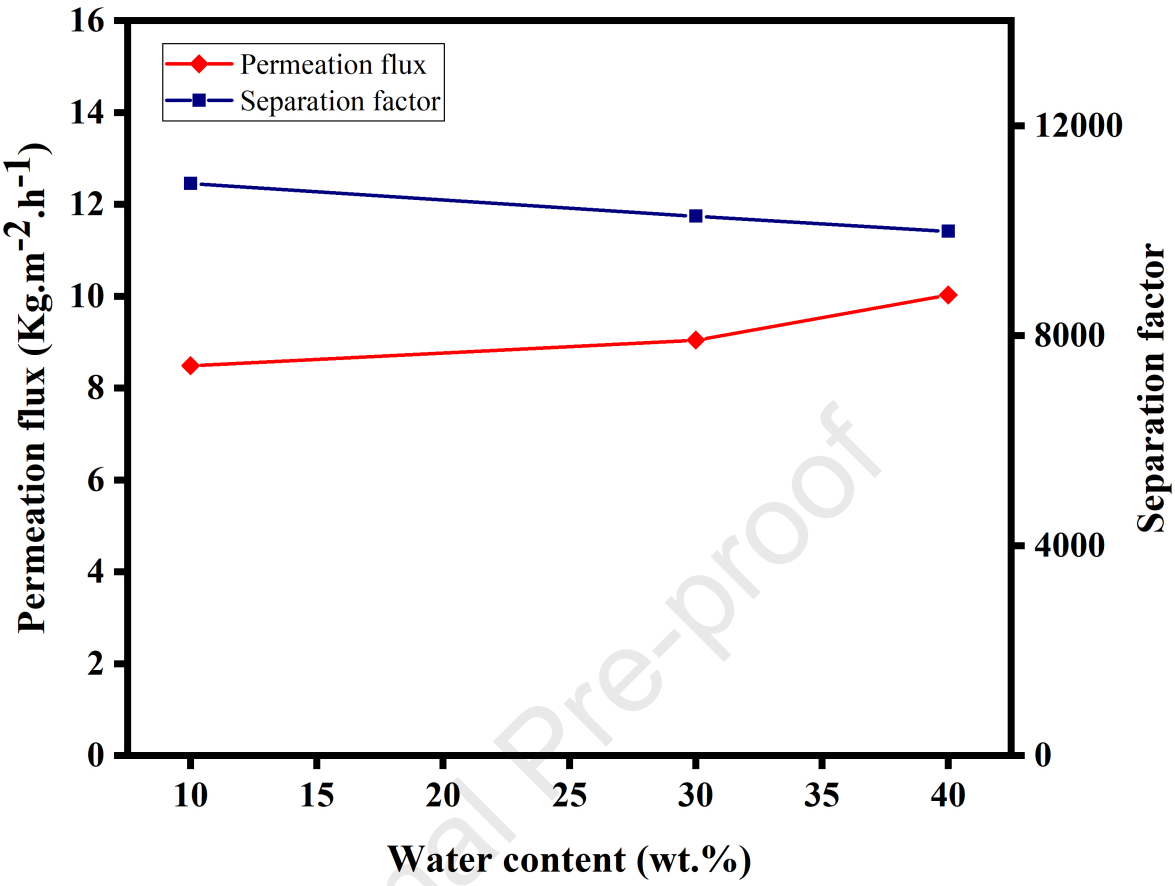

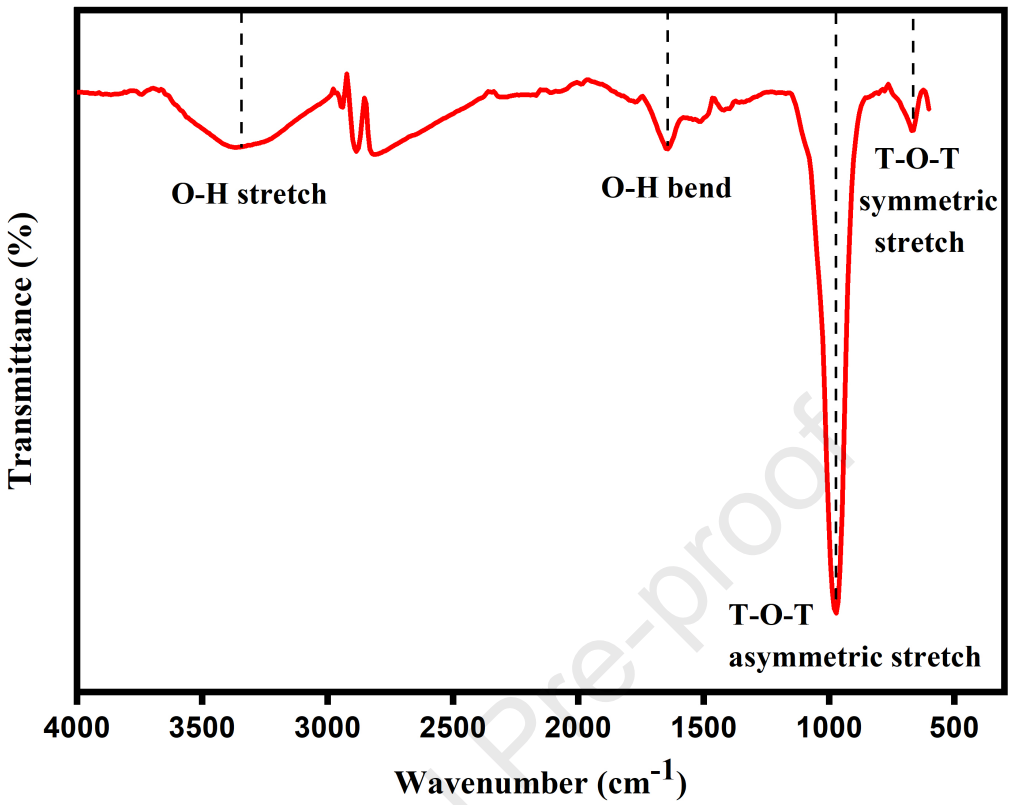

Highlights

- Low-cost NaA zeolite membrane with high permeation was prepared.
- Pure NaA zeolite synthesized at lower temperature of 60 °C.
- The membrane is efficient for dewatering of ethanol via pervaporation at 75 °C.
- High flux of 8.49 Kg m^{-2} h^{-1} and excellent separation factor are achieved

Conflict of interest

☑The authors declare that they have no known competing financial interests or personal relationships that could have appeared to influence the work reported in this paper.

☐ The authors declare the following financial interests/personal relationships which may be considered as potential competing interests:

None.